AD705634

Interim Report 69-2

AD

RCS OSD-1366

Research and Development Technical Report
ECOM 2-68 1-5

THE ENERGY BUDGET AT THE EARTH'S SURFACE: BASIC CONCEPTS OF SPECTRAL ANALYSIS BY DIGITAL MEANS

Contribution by:

B. A. Kimball

MICROCLIMATE INVESTIGATIONS
INTERIM REPORT 69-2

E. R. Lemon — Investigations Leader
U. S. DEPT. OF AGRICULTURE and
CORNELL UNIVERSITY

NOVEMBER 1969

DDC
RECEIVED
MAY 15 1970
C

This document has been approved for public release and sale; its distribution is unlimited.

ECOM
ELECTRONICS COMMAND
LABORATORY

CLEARINGHOUSE

U. S. Department of Agriculture
Ithaca, New York 14850

ACCESSION for
CFSTI WHITE SECTION ☑
DDC BUFF SECTION ☐
UNANNOUNCED ☐
JUSTIFICATION .....
.....
BY .....
DISTRIBUTION/AVAILABILITY CODES
DIST. AVAIL. and/or SPECIAL
1

NOTICES

Citation of trade names and names of manufacturers in this report is not to be construed as official Government indorsement or approval of commercial products or services referenced.

The findings of this report are not to be construed as an official Department of Army position unless so designated by other authorized documents.

Destroy this report when it is no longer needed. Do not return it to the originator.

Technical Report ECOM 2-68I-5
November 1969

Reports Control Symbol
OSD - 1366

THE ENERGY BUDGET AT THE EARTH'S SURFACE:

BASIC CONCEPTS OF SPECTRAL ANALYSIS BY DIGITAL MEANS

INTERIM REPORT 69-2

Cross Service Order 2 - 68
Task 1T0-61102-B53A-17

Prepared by

B. A. Kimball

of

Northeast Branch
Soil and Water Conservation Research Division
Agricultural Research Service
U. S. Department of Agriculture
Ithaca, New York

Report No. 406

In Cooperation With

N. Y. State College of Agriculture
Cornell University
Ithaca, New York

Research Report No. 870A

For

U. S. Army Electronics Command
Atmospheric Sciences Laboratory
Fort Huachuca, Arizona

PREFACE

This publication (Interim Report 69-2) forms the second part of two reports dealing with gas exchange from soil. Included here are pages 125-188 forming the appendix. We have chosen to make two reports because of the anticipated diversity of interest in them.

E. R. Lemon

TABLE OF CONTENTS

		Page
I.	Introduction	125
II.	One-dimensional spectral analysis	128
	1. Fourier series representation	128
	2. Relation of variance to spectral density function	132
	3. Relation of spectral density function to Fourier transform	139
	4. Relation of spectral density function to auto-covariance function	147
	5. Variability of the spectral estimates	152
	6. Aliasing	154
	7. Trends	156
III.	Cross-spectral analysis	157
IV.	Two-dimensional spectral analysis	164
	1. Fourier series representation	164
	2. Relation of variance to 2-D spectral density function	167
	3. Relation of 2-D spectral density function to Fourier transform	173
	4. Relation of 2-D spectral density function to 2-D auto-covariance function	175
V.	Use of cross-spectral density functions in 2-D analysis	178
	1. The assumptions of stationarity and spacial homogeneity	178
	2. Relationship between cross-spectral density function and 2-D spectral density function	181

Page

3. Relationship between cross-spectral density functions and 2-D auto-covariance functions 183

VI. Summary 185

VII. Literature Cited 187

LIST OF ILLUSTRATIONS

Figure		Page
A.2.1	Illustration of the sampling of p at the various times, t_j	129
A.2.2	Plot of Fourier line spectrum	135
A.2.3	Periodogram of $\frac{1}{\Delta f} 2\left\|C_n\right\|^2$ against f_n	137
A.2.4	Plot of spectral density function against frequency	138
A.2.5	The curve for calculation of a spectrum by hand	141
A.2.6	A spectrum	145
A.2.7	Three methods for plotting spectra of air pressure	146
A.2.8	The auto-covariance function for the curve in Fig. A.2.5	148
A.2.9	Illustration of how digital sampling may cause a high frequency component to alias and appear as a low frequency component	155
A.3.1	Coherence and phase spectrum for air pressure between a point on the ground surface in a field and another point downwind from the first	161
A.4.1	Illustration of coordinate system and notation for sampling p	165
A.4.2	Plot of Fourier line spectrum	169
A.4.3	Plot of 3-D "periodogram"	171
A.4.4	Contour surface of spectral density function, $s(f_n,k_m)$, plotted against frequency and wave number	172
A.5.1	Sampling scheme which can be used where p is statistically stationary and spacially homogeneous	179

Appendix

BASIC CONCEPTS OF SPECTRAL ANALYSIS BY DIGITAL MEANS

I. INTRODUCTION

A statistical technique that has helped meteorologists study wind and other fluctuating variables but which as yet has been rarely used by agronomists is spectral analysis. Spectral analysis is used to evaluate the contributions of different frequencies of the fluctuation to the total variance of an entity, such as wind velocity, which changes with time. A graph of the variance per frequency band forms a spectrum not unlike the more commonly known spectrum of light intensity versus wave length. Knowing the frequencies of the dominant modes of oscillation (or knowing that there are none) can help one to understand and visualize the physics of the transport processes mentioned in the first paragraph. Allen (1968), for instance, has used spectral analysis to study the eddy structure of wind in a Japanese larch canopy and found significant contributions to the variance of wind velocity by eddies the size of the tree spacing at mid-canopy heights. There was surprisingly little contribution from these eddies at the bottom of the canopy.

Spectral analysis can be used to study two or more fluctuating variables to determine the closeness of their relationship for different frequencies of change. Desjardins (1967), for instance, has compared the responses of various atmometers to open pan evaporation. He found that the variances were similar for periods of time longer than five days, but different for shorter periods, indicating that different physical factors must be in operation for the different instruments. Rodriguez-Iturbe and

Nordin (1969) used spectral analysis techniques to show the existence of strong correlations among annual oscillations in precipitation and run-off in the Pacific Coast region of the United States. The annual cycle of precipitation could be considered the same for observation stations up to 1000 km apart.

Spectral analysis was first developed for practical use by electrical engineers. Because the variance of a voltage across or a current through a unit resistance is proportional to the average power dissipation, the term power spectrum has often been used to refer to the spectrum of variance. Communication engineers have made much use of spectral analysis, and the theory and procedures of making spectral analysis are explained in much detail by Blackman and Tukey (1958). A much less sophisticated, but easily understood explanation of the underlying principles of spectrum analysis from the point of view of metecrology may be obtained from Panofsky and Brier (1965). Lumley and Panofsky (1964) present a much more sophisticated treatment from the same viewpoint. Jenkens and Watts (1968) present an excellent explanation of the principles from a statistician's point of view.

In 1965 Cooley and Tukey revealed a new algorithm for fast computation of Fourier transforms which has made spectral analysis much easier. An easily understood description of the new method is given by Brigham and Morrow (1967). More information may be obtained in the June 1967 issue of IEEE Transactions on Audio and Electroacoustics, vol. 15, no. 2, which was devoted entirely to the fast Fourier transform and how it relates to spectral analysis and other subjects.

The author has found all of the above references useful in understanding spectral analysis, but found none which developed the principles with reference to the new computational methods for persons who previously had little knowledge about spectrum analysis. This paper attempts to develop the concepts of spectral analysis for a reader who previously knows little about spectral analysis and whose background includes no more mathematics than basic calculus and statistics.

The orientation here will be toward the use of a digital computer to compute spectra from a series of samples of discrete data; therefore, the discrete forms of equations are used wherever possible. Spectra can be measured directly by electronic filtering of continuous electrical analog signals, but suitable analog signals cannot be obtained for many variables.

II. ONE-DIMENSIONAL SPECTRAL ANALYSIS

This section will discuss the fluctuation of an entity that changes with time. All of the concepts would apply equally well if the entity would change with some other variable, such as distance, but spectral analysis has been used more frequently with entities that change with time than with other variables, so this orientation will be used in this development. The term, one-dimensional, refers to the fact that the entity fluctuates only with one variable, time. Later, an entity that fluctuates with two variables, time and distance, will be examined, and the analysis will be referred to as two-dimensional spectral analysis.

1. Fourier series representation

Suppose some quantity, p (perhaps air pressure), a function of time, t, has been observed N times, where N is chosen to be odd for convenience, and that the observations have been spaced equally Δt units apart. Let the individual time of sampling be labelled $t_j = j\,\Delta t$ for $j = -\frac{(N-1)}{2}$, $-\frac{(N-3)}{2}$, ... -1, 0, 1, ... , $\frac{N-1}{2}$ so that the time origin is in the middle of the total sampling period, T. Note that $T = (N-1)\,\Delta t$. Figure A.1.1 illustrates the sampling scheme.

Since we are basically interested in evaluating the amplitude and frequency of the fluctuations in p, it is useful to describe p by a <u>Fourier series</u> of complex exponentials as in Equation A.2.1, where $i = \sqrt{-1}$.

$$p(t) = \sum_{n=-\infty}^{\infty} C_n \exp\left(\frac{i\,n\,2\,\pi\,t}{T}\right) \qquad \text{A.2.1}$$

Equation A.2.1 represents the continuous pressure between time -T/2 and +T/2 as a function of continuous time. The complex coefficients C_n may

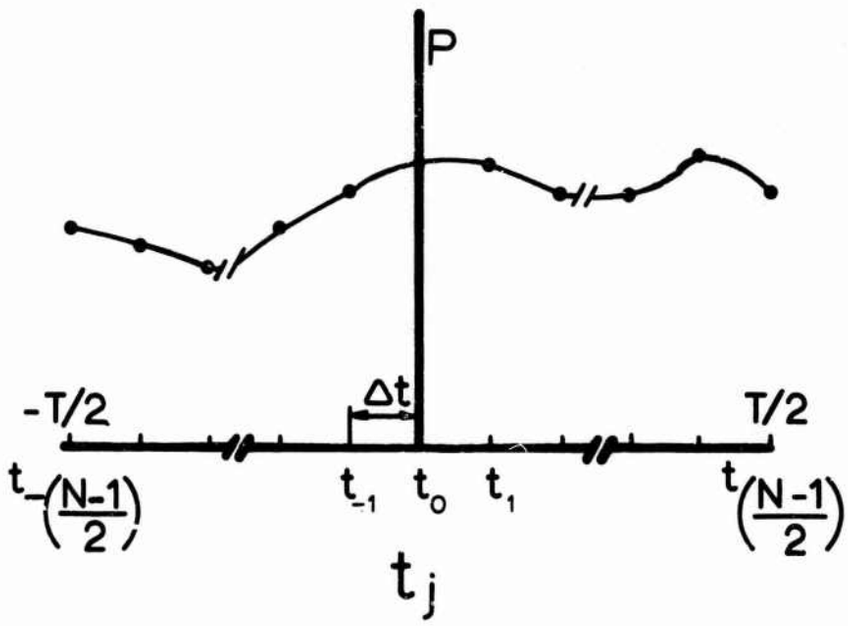

Figure A.2.1 Illustration of the sampling of p at the various times, t_j

be evaluated by multiplying both sides of Equation A.2.1 by $\exp(\frac{i\ q\ 2\ \pi\ t}{T})$ for q = ... -2, -1, 0, 1, 2 . . . . . and integrating from -T/2 to +T/2. Noting that

$$\int_{-T/2}^{T/2} \exp(\frac{i\ n\ 2\ \pi\ t}{T}) \quad \exp(\frac{i\ q\ 2\ \pi\ t}{T})\ dt$$

$$= T \text{ when } q = -n$$

$$= 0 \text{ when } q \neq -n \qquad \text{A.2.2}$$

one obtains

$$C_n = 1/T \quad \int_{-T/2}^{T/2} p(t)\ \exp(\frac{-i\ n\ 2\ \pi\ t}{T})\ dt \qquad \text{A.2.3}$$

Equations A.2.1 and A.2.3 are for continuous variables. To put Equation A.2.1 in a form for handling a finite number of discrete observations, one writes

$$p(t_j) = \sum_{n=\frac{-(N-1)}{2}}^{\frac{N-1}{2}} C_n \quad \exp(\frac{i\ n\ 2\ \pi\ t_j}{T}) \qquad \text{A.2.4}$$

Equation A.2.3 is discretized by numerical integration with the rectangle rule to give

$$C_n = \frac{\Delta t}{T} \sum_{j=\frac{-(N-1)}{2}}^{\frac{N-1}{2}} p(t_j) \quad \exp(\frac{-i\ n\ 2\ \pi\ t_j}{T}) \qquad \text{A.2.5}$$

Each pair of terms in Equation A.2.4 corresponding to n and -n represents a particular harmonic in the fluctuations of p. Also n denotes the frequency of the harmonic because it measures the number of complete cycles the nth harmonic executes in time T. The particular limits on n arise because of an assumption inherent in making the sampled points of p

substitute for the real, continuous p. This assumption is that the sample interval, Δt, is small enough so that there are no undetected high frequency fluctuations in p between the points. As discussed by Blackman and Tukey (1958, p. 30), the highest frequency or harmonic which can be detected when sampling at discrete intervals is given by $1/(2\Delta t)$, which corresponds to $n = \pm \frac{N-1}{2}$. If p has higher frequency fluctuations, the data will be aliased. This problem is discussed more fully later. The term corresponding to $n = 0$ is the mean of p. The terms corresponding to $n = \pm 1$ represent the first (or fundamental) harmonic which has a frequency of $1/T$. It is the lowest frequency of fluctuation in p which can be distinguished, and if lower frequencies are present, such as is the case when there is a trend in p, corrections must be made, as will be discussed later.

Note that, in general, the C_n are complex. If one writes Equation A.2.4 in the form

$$p(t_j) = C_o + \sum_{n=1}^{\frac{N-1}{2}} [C_n \exp(\frac{i\ n\ 2\ \pi\ t_j}{T}) + C_{-n} \exp(\frac{-i\ n\ 2\ \pi\ t_j}{T}] \qquad \text{A.2.6}$$

and uses the Euler equations

$$e^{i\theta} = \cos\theta + i \sin\theta \qquad \text{A.2.7}$$

$$e^{-i\theta} = \cos\theta - i \sin\theta \quad , \qquad \text{A.2.8}$$

Equation A.2.4 is changed to a Fourier series of sines and cosines.

$$p(t_j) = C_o + \sum_{n=1}^{\frac{N-1}{2}} [(C_n + C_{-n}) \cos(\frac{n\ 2\ \pi\ t_j}{T}) +$$

$$i(C_n - C_{-n}) \sin(\frac{n\ 2\ \pi\ t_j}{T})] \qquad \text{A.2.9}$$

Then, if one defines

$$a_o = 2C_o \qquad \text{A.2.10}$$

$$a_n = C_n + C_{-n} \qquad \text{A.2.11}$$

$$b_n = i\,(C_n - C_{-n}) \qquad \text{A.2.12}$$

Equation A.2.9 becomes the more familiar

$$p(t_j) = \frac{a_o}{2} + \sum_{n=1}^{\frac{N-1}{2}} \left[a_n \cos\left(\frac{n\,2\,\pi\,t_j}{T}\right) + b_n \sin\left(\frac{n\,2\,\pi\,t_j}{T}\right)\right] \qquad \text{A.2.13}$$

which will not be used here because the Fourier transforms discussed later in the paper are more easily handled by the series of exponentials.

Also, note that by rearranging Equations A.2.11 and A.2.12,

$$C_n = \frac{a_n}{2} - i\,\frac{b_n}{2} \qquad \text{A.2.14}$$

and

$$C_{-n} = \frac{a_n}{2} + i\,\frac{b_n}{2} \qquad \text{A.2.15}$$

so that C_n and C_{-n} are seen to be complex conjugates, a result which is useful later.

2. Relation of variance to spectral density function

A common statistical parameter used to measure variability is the <u>variance</u>, s^2. It is defined

$$s^2 = \frac{1}{N-1} \sum_{j=\frac{-(N-1)}{2}}^{\frac{N-1}{2}} [p(t_j) - \bar{p}]^2 \qquad \text{A.2.16}$$

where the $p(t_j)$ are the observations of p, N is the number of observations

and $\bar{p}$ is the mean of $p(t_j)$. The limits of summation are $\pm\frac{(N-1)}{2}$, which will be the limits of summation from the point on, unless noted otherwise. If Equation A.2.4 is used to substitute for $p(t_j)$ in Equation A.2.16, the variance becomes explicitly expressed as a function of the harmonics of p. Remembering that $\bar{p} = C_o$ and $\frac{1}{N-1} = \frac{\Delta t}{T}$, one obtains

$$s^2 = \frac{\Delta t}{T} \sum_j \left[\sum_n \left[C_n \exp\left(\frac{i\ n\ 2\ \pi\ t_j}{T}\right)\right] - C_o\right]^2 \qquad \text{A.2.17}$$

Equation A.2.17 is the numerical form for the following integral equation.

$$s^2 = 1/T \int_{-T/2}^{T/2} \left[\sum_n \left[C_n \exp\left(\frac{i\ n\ 2\ \pi\ t}{T}\right)\right] - C_o\right]^2 dt \qquad \text{A.2.18}$$

If the summation is written out in a series, and if the squaring is performed on the series, the following expression is obtained

$$\begin{aligned} s^2 = 1/T \int_{-T/2}^{T/2} \Big[& C^2_{\frac{-(N-1)}{2}} \exp\left(\frac{-i(N-1)\ 2\ \pi\ t}{T}\right) + 2C_{\frac{-(N-1)}{2}} C_{\frac{-(N-3)}{2}} \exp\left(\frac{-i(N-2)\ 2\pi\ t}{T}\right) \\ & + \ldots\ldots\ 2C_{\frac{-(N-1)}{2}}\ C_{\frac{N-1}{2}} + \ldots\ldots\ldots\ldots\ldots\ldots \\ & + C^2_{-n} \exp\left(\frac{-i\ n\ 4\ \pi\ t}{T}\right) + 2C_{-n} C_{-(n+1)} \exp\left(\frac{-i(2n+1)\ 2\ \pi\ t}{T}\right) \\ & + \ldots\ldots\ldots + 2C_{-n} C_n + \ldots\ldots + C^2_n \exp\left(\frac{i\ n\ 4\ \pi\ t}{T}\right) \\ & + \ldots\ldots\ldots\ldots\ldots\ldots\ldots\ldots\ldots\ldots \\ & + \ldots\ldots\ldots\ldots\ldots\ldots\ldots\ldots\ldots\ldots \Big]\ dt \end{aligned}$$

A.2.19

Recalling Equation A.2.2, the variance is seen to be equal to a sum of squared moduli of coefficients.

$$s^2 = 2 \sum_{n=1}^{\frac{N-1}{2}} C_{-n} C_n = 2 \sum_{n=1}^{\frac{N-1}{2}} |C_n|^2 \qquad \text{A.2.20}$$

The vertical bars denote the modulus, which is obtained by multiplying C_n by its complex conjugate, C_{-n}, and taking the square root of the product. In Equation A.2.20 the variance is expressed as a function of the amplitudes of the harmonics from 1 to $\frac{N-1}{2}$. The variance may also be considered as a sum over negative and positive harmonics since the modulus is an even function. Thus,

$$s^2 = -C_o^2 + \sum_{n = -\frac{(N-1)}{2}}^{\frac{N-1}{2}} |C_n|^2 \qquad \text{A.2.21}$$

The form in Equation A.2.20 is most common, however.

Now, if one defines

$$f_n = n/T \qquad \text{A.2.22}$$

and

$$\Delta f = 1/T \qquad \text{A.2.23}$$

and plots $2|C_n|^2$ against f_n we obtain the <u>Fourier line spectrum</u> shown in Figure A.2.2. The f_n represent the frequencies of the harmonics, and Δf represents the frequency increment between successive harmonics. Thus, the "curve" is a series of lines of height $2|C_n|^2$ spaced Δf units apart.

If one assumes that heights of $2|C_n|^2$ are distributed uniformly over the frequency band from $f_n - \Delta f$ to f_n, a histogram may be obtained where the height of the bands is determined from

$$2|C_n|^2 = (\text{height})\ (\Delta f) \qquad \text{A.2.24}$$

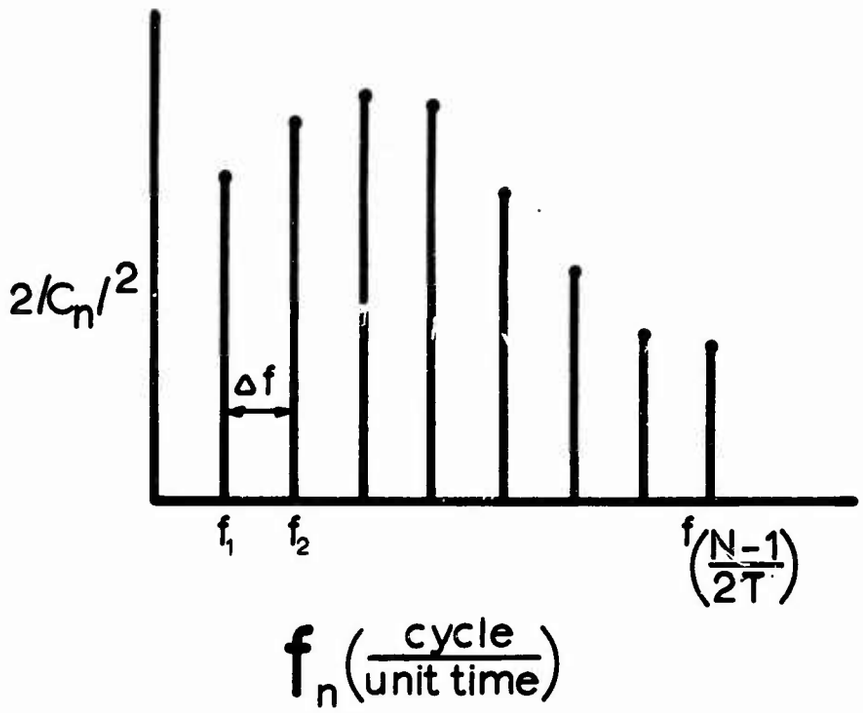

Figure A.2.2 Plot of Fourier line spectrum

or $$\text{height} = \frac{1}{\Delta f}\ 2|C_n|^2 \qquad \text{A.2.25}$$

A plot of $\frac{1}{\Delta f}\ 2|C_n|^2$ against f_n is shown in Figure A.2.3.

Figure A.2.3. is called a periodogram in spite of the fact that the axis is frequency and not time. The total area of the rectangles equals the total variance. As the period, T, increases, Δf decreases by an inverse proportion, and the rectangles in the histogram of Figure A.3 become narrower. In the limit as $T \to \infty$, Δf tends to zero, and the rectangles become so dense that their discrete upper edges approach a smooth curve. The limiting smooth curve is the <u>spectral density function</u>, s(f), and the plot of it against frequency in Figure A.2.4 represents a <u>variance spectrum</u> or <u>power spectrum</u>. In practice, of course, one does not have an infinite sampling time, as is implied by letting $T \to \infty$, so one must approximate the spectral density function, using finite sampling times and finite Δf's.

The practical spectral density function, now defined as

$$s(f_n) = \frac{1}{\Delta f}\ 2|C_n|^2 \qquad n = 1, 2, \ldots\ldots\ldots \frac{N-1}{2} \qquad \text{A.2.26}$$

represents the variance in p per frequency increment. The total area under the curve represents the total variance. The graph can be normalized, if desired, by dividing $s(f_n)$ by the total variance calculated directly from Equation A.2.16. The normalized graph will always have the area under the curve equal to 1.0.

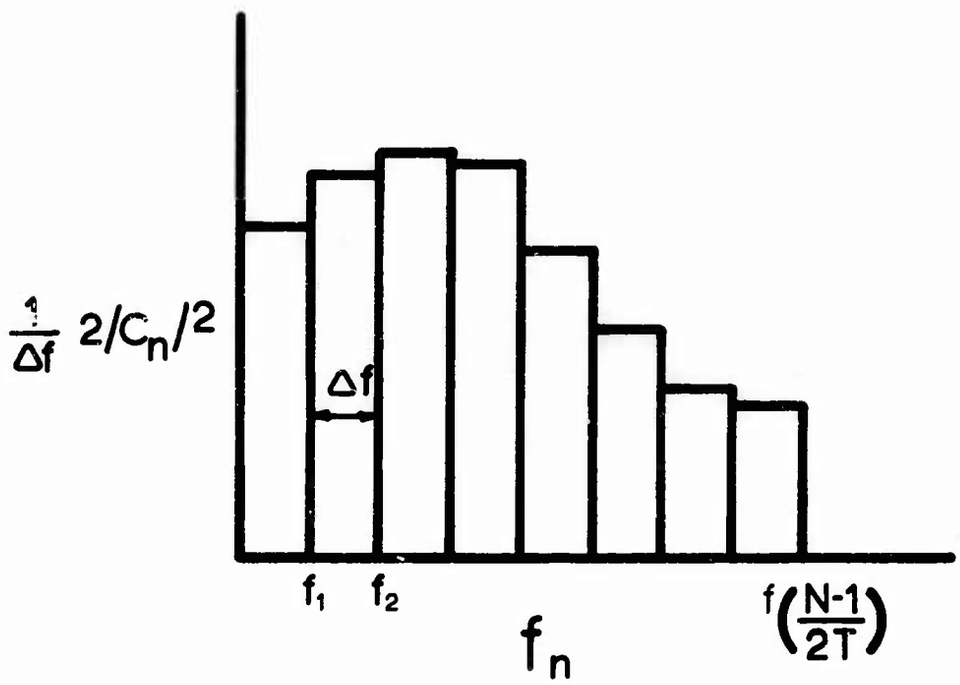

Figure A.2.3 Periodogram of $\frac{1}{\Delta f}\ 2|C_n|^2$ against f_n

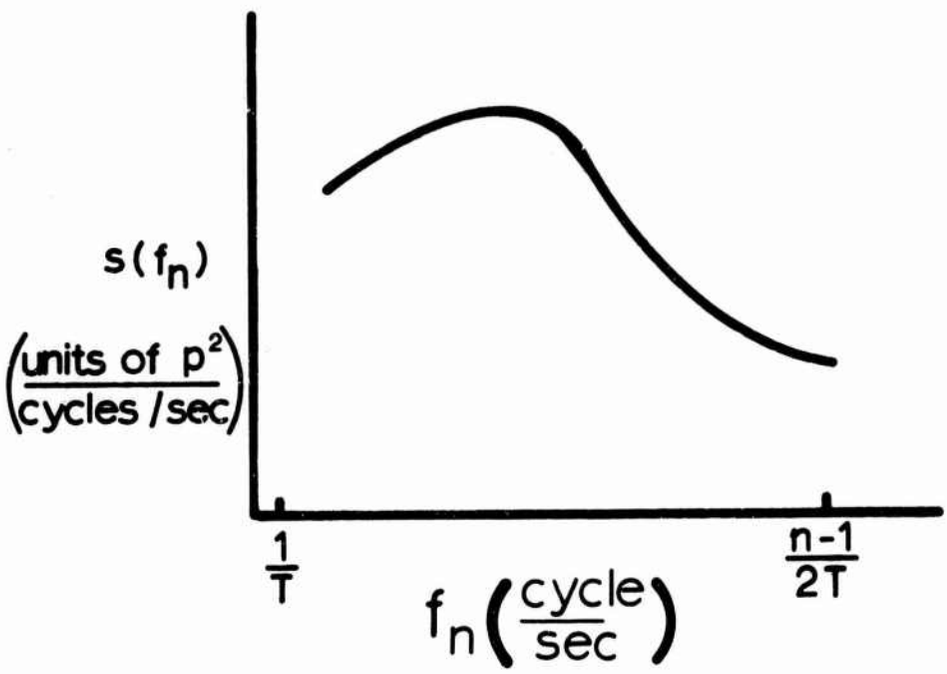

Figure A.2.4 Plot of spectral density function against frequency

3. Relation of spectral density function to Fourier transform

Using Equations A.2.22 and A.2.23, Equations A.2.24 and A.2.25 may be rewritten in the forms:

$$p(t_j) = \sum_n C_n \exp(i2\pi f_n t_j) \qquad \text{A.2.27}$$

and

$$C_n = \Delta t \Delta f \sum_j p(t_j)\exp(-i2\pi f_n t_j) \qquad \text{A.2.28}$$

Substituting Equation A.2.28 in A.2.27, one obtains

$$p(t_j) = \sum_n [\Delta t \Delta f \sum_j p(t_j)\exp(-i2\pi f_n t_j)] \exp(i2\pi f_n t_j) \qquad \text{A.2.29}$$

If one now defines

$$S(f_n) = \Delta t \sum_{j=-\frac{(N-1)}{2}}^{\frac{N-1}{2}} p(t_j)\exp(-i2\pi f_n t_j) \ , \qquad \text{A.2.30}$$

where the $S(f_n)$ are commonly called Fourier coefficients,

then $$p(t_j) = \Delta f \sum_{n=-\frac{(N-1)}{2}}^{\frac{N-1}{2}} S(f_n)\exp(i2\pi f_n t_j) \qquad \text{A.2.31}$$

$S(f_n)$ and $p(t_j)$ form a discrete <u>Fourier transform pair</u>. Using the computer technique of <u>fast Fourier transformation</u>, as described by Brigham and Morrow (1967), $S(f_n)$ can be rapidly computed from the set of data points (t_j). Alternatively, if the $S(f_n)$ are known, the $p(t_j)$ can be computed from the $S(f_n)$.

The significance of the $S(f_n)$ may be realized by noting that

$$S(f_n) = \frac{C_n}{\Delta f} \qquad \text{A.2.32}$$

and remembering that C_n and C_{-n} are complex conjugates. Then if $S(f_n)$ is multiplied by its complex conjugate, $S(-f_n)$, one obtains

$$S(f_n)\cdot S(-f_n) = |S(f_n)|^2 = \frac{C_n}{\Delta f}\cdot\frac{C_{-n}}{\Delta f} = \frac{1}{(\Delta f)^2}\,|C_n|^2 \qquad \text{A.2.33}$$

where the vertical bars denote modulus.

The spectral density function defined by Equation A.2.26 is seen to be equal to twice the squared modulus of the Fourier transform of the date points times the frequency increment.

$$s(f_n) = 2\,\Delta f|S(f_n)|^2\ ,\ n = 1, 2, \ldots \frac{N-1}{2} \qquad \text{A.2.34}$$

Thus, the spectral density function may be computed by a fast Fourier transform of the data for $n = 1, 2 \ldots \frac{N-1}{2}$ and then multiplying each of the $S(f_n)$ by its complex conjugate times $2\Delta f$.

An example of the use of Equations A.2.30 and A.2.34 is provided by the hand calculation of the spectrum for the simple curve illustrated in Figure A.2.5. Noting that $\Delta t = 0.1$ sec, that $N = 17$, and that $f_n t_j = nj/(N - 1)$, one writes

$$s(f_n) = (0.1)\sum_{j=-8}^{+8} p(t_j)\left(\cos\frac{2\pi nj}{16} - i\,\sin\frac{2\pi nj}{16}\right)$$

The next step is to compute all the values of $\cos\frac{2\pi nj}{16}$ and $\sin\frac{2\pi nj}{16}$ for $j = -8 \ldots +8$ and $n = 1$, as has been done in the third and fourth columns of Table A.2.1. In the fifth and sixth columns, the cosine and sine values are multiplied by the corresponding $p(t_j)$ and summed on j. The calculation of $S(f_1)$ and $s(f_1)$ is illustrated at the bottom of Table A.2.1. The process is continued for $n = 2$, as shown in the table, up to $n = 8$ to

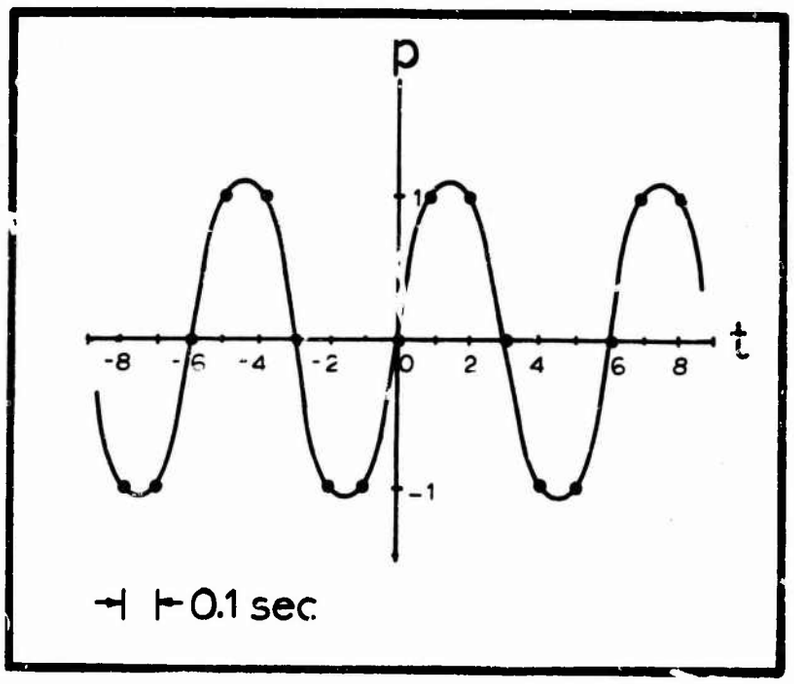

Figure A.2.5 The curve for calculation of a spectrum by hand

Table A.2.1 Calculation of the spectral density for n = 1, 2 for the curve in Fig. A.2.5

		n = 1				n = 2			
j	$p(t_j)$ (μbar)	$\cos\frac{2\pi nj}{16}$	$\sin\frac{2\pi nj}{16}$	p cos	p sin	$\cos\frac{2\pi nj}{16}$	$\sin\frac{2\pi nj}{16}$	p cos	p sin
-8	-1	-1.000	0.000	1.000	0.000	1.000	0.000	-1.000	0.000
-7	-1	-0.924	-0.383	0.924	0.383	0.707	0.707	-0.707	-0.707
-6	0	-0.707	-0.707	0.000	0.000	0.000	1.000	0.000	0.000
-5	1	-0.383	-0.924	-0.383	-0.924	-0.707	0.707	-0.707	0.707
-4	1	0.000	-1.000	0.000	-1.000	-1.000	0.000	-1.000	0.000
-3	0	0.383	-0.924	0.000	0.000	-0.707	-0.707	0.000	0.000
-2	-1	0.707	-0.707	-0.707	0.707	0.000	-1.000	0.000	1.000
-1	-1	0.923	-0.383	-0.924	0.383	0.707	-0.707	-0.707	0.707
0	0	1.000	0.000	0.000	0.000	1.000	0.000	0.000	0.000
1	1	0.923	0.383	0.923	0.383	0.707	0.707	0.707	0.707
2	1	0.707	0.707	0.707	0.707	0.000	1.000	0.000	1.000
3	0	0.383	0.923	0.000	0.000	-0.707	0.707	0.000	0.000

Table A.2.1 (cont.)

4	-1	0.000	1.000	0.000	-1.000	-1.000	0.000	1.000	0.000
5	-1	-0.383	0.924	0.383	-0.924	-0.707	-0.707	0.707	0.707
6	0	-0.707	0.707	0.000	0.000	0.000	-1.000	0.000	0.000
7	1	-0.924	0.383	-0.924	0.383	-0.707	-0.707	-0.707	-0.707
8	1	-1.000	0.000	-1.000	0.000	1.000	0.000	1.000	0.000
Sum	0.0			0.000	-0.902			0.000	3.414

$\bar{p} = 0.0$

$$S(f_1) = (0.1) \sum_{j=-8}^{8} \left[p(t_j) \cos\frac{2\pi(1)j}{16} - i\, p(t_j) \sin\frac{2\pi(1)j}{16} \right]$$

$$= (0.1)\,[0.000 - i(-0.902)]$$

$$= 0.000 + i(0.0902) \quad [\ \mu\text{bar sec}]$$

$$S(f_2) = 0.000 - i(0.3414)$$

$$s(f_2) = 0.145$$

$$f_2 = (2)(\Delta f)$$

$$= 1.25 \text{ cycle/sec}$$

$$s^2 = \frac{1}{N-1} \sum_{j=1}^{N} (p - \bar{p})^2$$

$$= 12.0$$

$$\Delta f = 1/1.6 \text{ sec}$$

$$= 0.625 \text{ cycle/sec}$$

$$s(f_1) = 2\Delta f\, |S(f_1)|^2$$

$$= 2\left(\frac{1}{1.6 \text{ sec}}\right) [0.000 + i(0.0902)]\,[0.000 - i(0.0902)]$$

$$= 0.0102\ [\mu\text{bar}^2/\text{cycle/sec}]$$

$$f_1 = 0.625 \text{ cycle/sec}$$

obtain the spectrum illustrated in Fig. A.2.6. The spectrum shows a peak at a frequency of 1.88 cycle/sec as one would predict from the distinct repetition near this frequency in the original data.

The spectrum in Figure A.2.6 is plotted with a linear scale for both axis. The area under each portion of the spectral density curve is the contribution of that corresponding frequency to the variance, and the total area is equal to the total variance. Very often in practice, however, a worker will be studying a variable whose spectrum covers a range of several orders of magnitude on both the frequency and spectral density axis. In such a case, a linear plot of the spectrum can obscure much of the detail, so a log-log plot is often used. Although the area under the curve is no longer equal to the total variance, a log-log plot has the advantage of covering wide ranges and of presenting as a straight line any spectrum which obeys a power law, such as isotropic turbulence in a stream of air. A third method of presenting spectra and a method which is often used, particularly in meteorology, is to plot f s(f) against log f. Since

$$\text{Area} = \int s(f)\, df = \int f\, s(f)\, d(\log f)$$

the area under the curve is preserved, and one can still observe the relative contribution of different frequency bands to the total variance. Wide ranges of spectral density and frequency can also be presented. In Figure A.2.7, the three methods of presenting spectra are illustrated for a spectrum of air pressure at the ground surface obtained by the author.

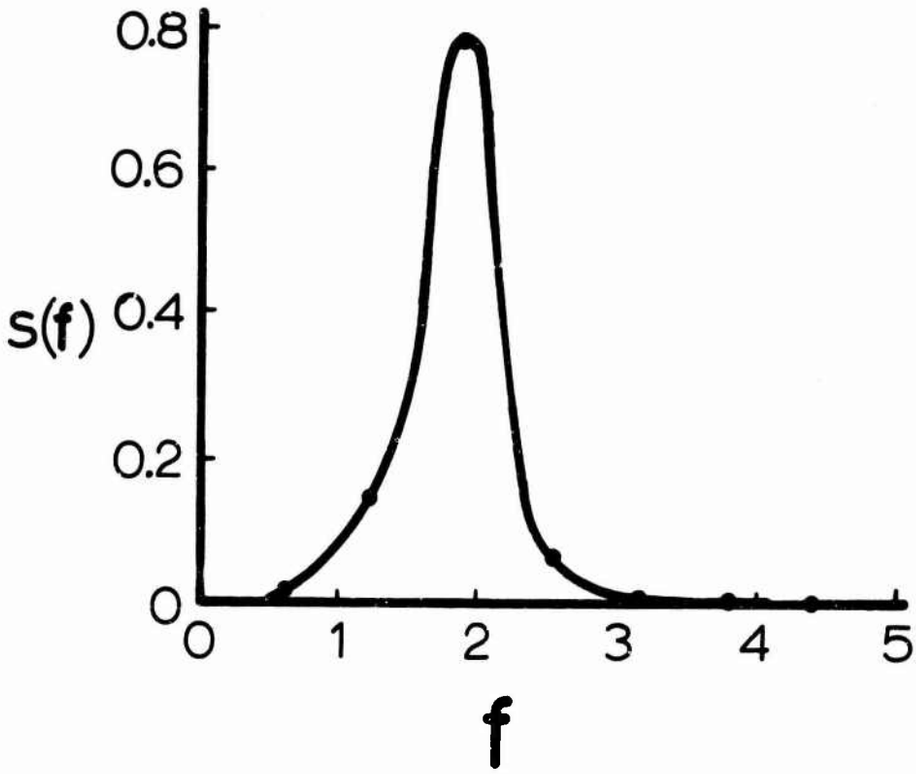

Figure A.2.6 A spectrum

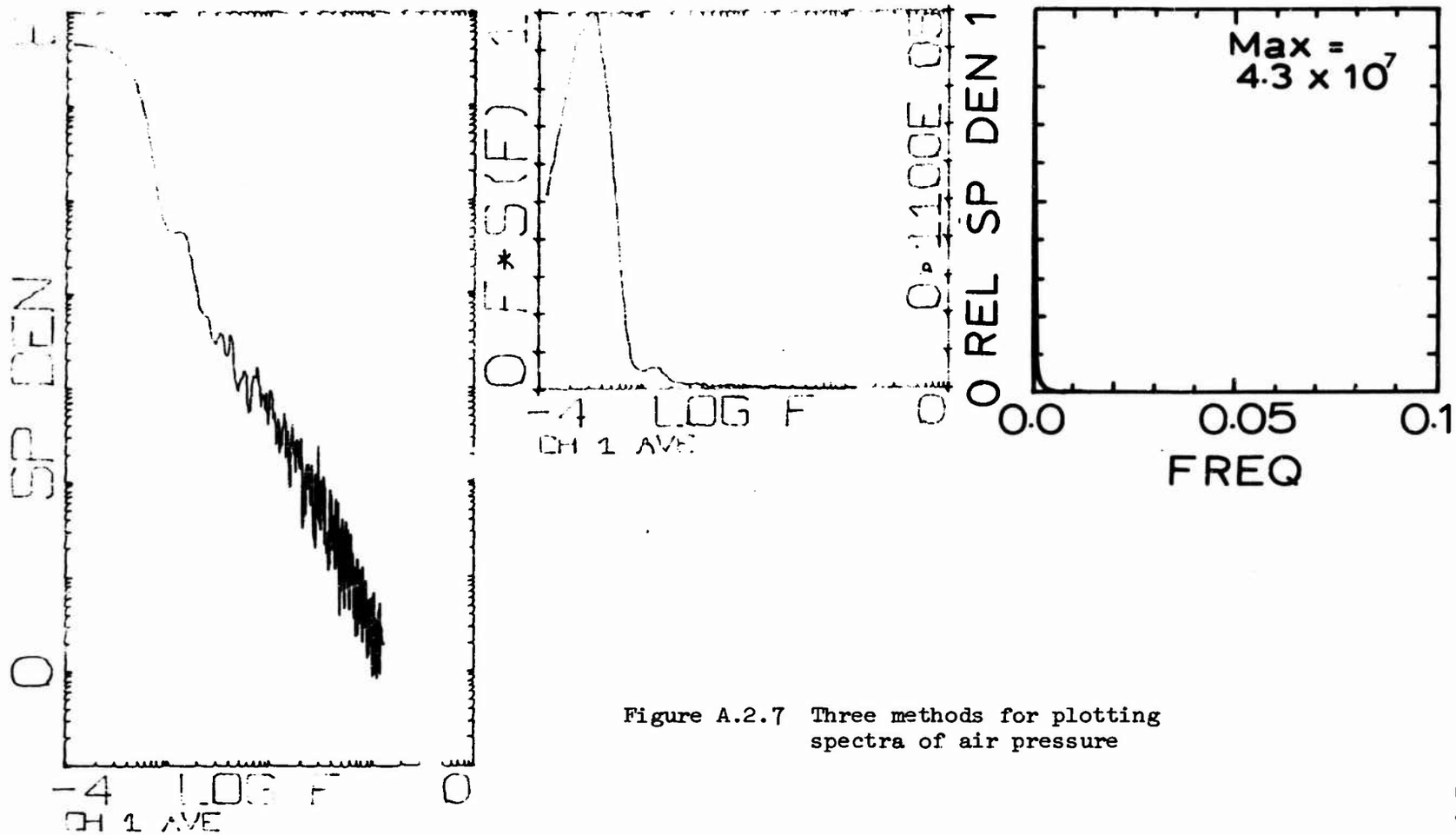

Figure A.2.7 Three methods for plotting spectra of air pressure

4. Relation of spectral density function to autocovariance function

The <u>autocovariance function</u>, $R(\tau_u)$, is defined by

$$R(\tau_u) = \frac{1}{N-1-u} \sum_{j=-\frac{(N-1-u)}{2}}^{\frac{N-1-u}{2}} [p(t_j) - \bar{p}]\,[p(t_j + \tau_u) - \bar{p}] \qquad \text{A.2.35}$$

where the bar denotes the mean. As the name implies, the autocovariance function expresses a covariance of $p(t_j)$ with itself. The τ_u represents a lag in time, and usually it is an integer multiple of Δt, i.e., $\tau_u = u\Delta t$ where u is an integer. Thus, $R(\tau_u)$ is the covariance of $p(t_j)$ with itself τ_u units of time later. It is computed by multiplying (after subtraction of the mean) each observation of $p(t_j)$ by another observation of $p(t_j)$ taken a time τ_u later (or earlier for negative τ_u), then summing all the lagged products and dividing by the number of products. For $\tau_u = 0$, $R(\tau_u)$ is identical with the usual variance function defined by Equation A.2.16, and very often the autocovariance function is normalized by dividing it by the usual variance. The normalized autocovariance function is called the autocorrelation function which varies only between ±1. A plot of autocovariance for the curve of Figure A.2.5 is shown in Figure A.2.8. The autocovariance is seen to be large and positive at u = 0 when the curve agrees perfectly with itself, small at u = 2 when the curve does not correspond with itself, large and negative at u = 3 when the positive peaks of the curve are opposite the negative peaks, and large and positive at u = 6 when all peaks correspond. When N>>u and $\bar{p} = 0$ (the data can be adjusted to give a zero mean, if necessary), Equation A.2.35 becomes

$$R(\tau_u) = \frac{1}{N-1} \sum_{j=-\frac{(N-1)}{2}}^{\frac{N-1}{2}} p(t_j)\, p(t_j + \tau_u) \qquad \text{A.2.36}$$

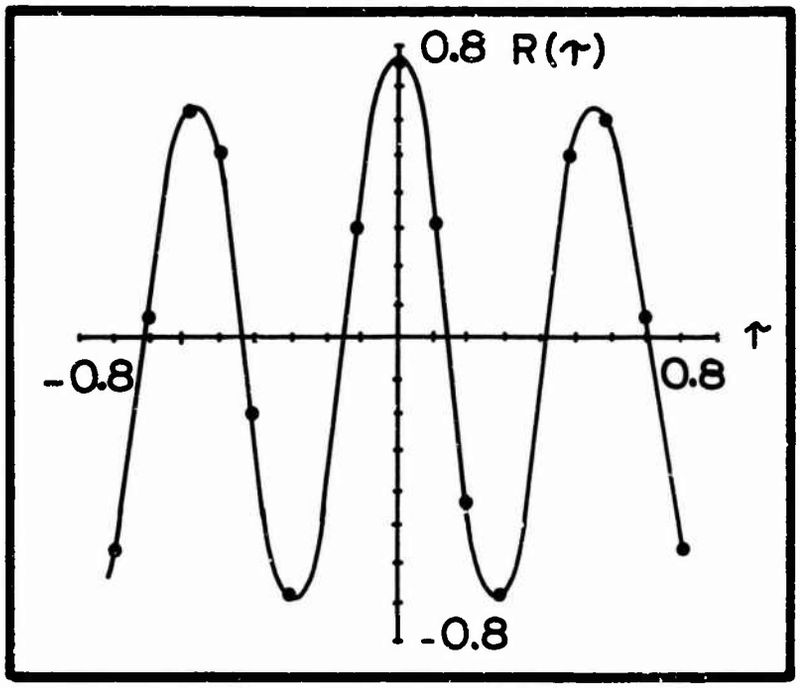

Figure A.2.8 The auto-covariance function for the curve in Fig. A.2.5

Equation A.2.36 will be used shortly.

The autocovariance function is useful because it illustrates the lengths of time for which a variable can be expected to be correlated with itself. It is useful also because it happens to be the Fourier transform of the spectral density function. A rigorous proof of this fact, as given by Blackman and Tukey (1958, p. 72), is possible only for continuous variables extending over infinite ranges. However, a demonstration of the basic idea can be given by using the discrete equations already developed. First, consider the concept of discrete convolution, which is somewhat analogous to the convolution of continuous functions described by Blackman and Tukey. Let

$$S(f_n) = \Delta t \sum_{j = -\frac{(N-1)}{2}}^{\frac{N-1}{2}} p(t_j) \exp(-i2\pi f_n t_j) \qquad \text{A.2.37}$$

and

$$p(t_j) = \Delta f \sum_{n = -\frac{(N-1)}{2}}^{\frac{N-1}{2}} S(t_j) \exp(i2\pi f_n t_j) \qquad \text{A.2.38}$$

describe a Fourier transform pair. Now let $S_b(f_n) = S(-f_n) \cdot S(f_n)$, and let the Fourier transform of $S_b(f_n)$ be denoted $B(\tau_u)$.

By Equation A.2.38

$$B(\tau_u) = \Delta f \sum_n S_b(f_n) \exp(i2\pi f_n \tau_u) = \Delta f \sum_n S(-f_n)\, S(f_n) \exp(i2\pi f_n \tau_u) \qquad \text{A.2.39}$$

Then, using Equation A.2.37 to substitute for $S(-f_n)$

$$B(\tau_u) = \Delta f \sum_n [\Delta t \sum_j p(t_j) \exp(i2\pi f_n t_j)]\, S(f_n) \exp(i2\pi f_n \tau_u) \qquad \text{A.2.40}$$

By reversing the order of summation, one obtains

$$B(\tau_u) = \Delta t \sum_j [\Delta f \sum_n S(f_n) \exp(i2\pi f_n(t_j + \tau_u))] \, p(t_j) \qquad \text{A.2.41}$$

Using Equation A.2.38, a substitution may be made for the expression in brackets, so that Equation A.2.41 becomes

$$B(\tau_u) = \Delta t \sum_{j = -\frac{(N-1)}{2}}^{\frac{N-1}{2}} p(t_j) \, p(t_j + \tau_u) \qquad \text{A.2.42}$$

Recalling that $T = (N-1)\,\Delta t$, $R(\tau_u)$ in Equation A.2.36 is seen to be equal to the expression for $B(\tau_u)$ given in Equation A.2.42 divided by T. Now recall that $B(\tau_u)$ was defined in Equation A.2.39 as the Fourier transform of $S(-f_n)\,S(f_n)$. Since $S(-f_n)$ is the complex conjugate of $S(f_n)$, $B(\tau_u)$ is the Fourier transform of $|S(f_n)|^2$. Using Equation A.2.21 for $C_o = \bar{p} = 0$, the relation between the spectral density function and $|S(f_n)|^2$ is

$$s(f_n) = \Delta f |S(f_n)|^2, \; n = -\frac{(N-1)}{2}, -\frac{(N-3)}{2}, \ldots, -1, 0, 1, \ldots \frac{N-1}{2} \qquad \text{A.2.43}$$

Therefore, using Equation A.2.43 and the fact that $R(\tau_u) = \Delta f$ $B(\tau_u)$, one obtains

$$R(\tau_u) = \Delta f \sum_{n = -\frac{(N-1)}{2}}^{\frac{N-1}{2}} s(f_n) \exp(i2\pi f_n \tau_u) \qquad \text{A.2.44}$$

which states that the autocovariance function is the Fourier transform of

the spectral density function. Due to the reciprocal nature of the Fourier transform pairs, $s(f_n)$ must also be the Fourier transform of $R(\tau_u)$, i.e.,

$$s(f_n) = \Delta t \sum_{u=-\frac{(N-1)}{2}}^{\frac{N-1}{2}} R(\tau_u) \exp(-i2\pi f_n \tau_u) \qquad \text{A.2.45}$$

During the past, the standard procedure for computing the spectral density function for a set of data points involved calculating the autocovariance functions first. Using Equation A.2.35 values of the autocovariance function were computed for lags covering about one-tenth of the total observation period. The spectral density function was then computed from Equation A.2.45 for the number of lags available. The development of the fast Fourier transform technique by Cooley and Tukey (1965) has made another approach computationally advantageous. First, the $S(f_n)$ are computed directly from the data using Equation A.2.30 for $n = 1, 2, \ldots \frac{N-1}{2}$. Each $S(f_n)$ is then multiplied by twice its complex conjugate and the spectral density function is obtained from Equation A.2.34.

Also, as explained by Stockham (1966), the autocovariance function now may be obtained most easily not from lagged products but by a second fast Fourier transformation. After the spectral density function is obtained, the transformation given by Equation A.2.44 is used to compute the autocovariance function from the spectral density function. However, it is not the usual autocovariance function but a circular autocovariance whereby overlapping values at the end of the summation interval for the lagged products are shifted around to the other end. This is why u goes from $-\frac{(N-1)}{2}$ to $\frac{(N-1)}{2}$ in Equations A.2.44 and A.2.45.

Since from Equation A.2.43, $s(f_n)$ can be seen to be an even function of f_n, and since from Equation A.2.36, $R(\tau_u)$ can be seen to be an even function of τ_u, the summation in A.2.44 and A.2.45 need be carried only over half the ranges. Thus,

$$R(\tau_u) = \Delta f \left[s(f_o) + 2 \sum_{n=1}^{\frac{N-1}{2}} s(f_n) \exp(i2\pi f_n \tau_u)\right] \qquad \text{A.2.46}$$

and

$$s(f_n) = \Delta t \left[R(\tau_o) + 2 \sum_{u=1}^{\frac{N-1}{2}} R(\tau_u) \exp(-i2\pi f_n \tau_u)\right] \qquad \text{A.2.47}$$

5. Variability of the spectral estimates

The experience of many investigators, particularly with meteorological data, has shown that the spectral density estimates calculated from Equation A.2.34 may scatter widely and also that the spectra from two different portions of the same time series may differ. These anomalies are now regarded to be due mostly to sampling error, and methods are available to obtain the underlying "smooth" spectrum. The traditional method described by Blackman and Tukey (1958) has been to calculate the autocovariance function for lags extending over approximately one-tenth of the total sampling period and then obtain the spectrum from a Fourier transform of the autocovariance function. Since the lags extend only over one-tenth of the total period, the computation is essentially an averaging and smoothing process, and a smoother spectrum is obtained. Additional smoothing is obtained by forming new estimates from weighted averages. i.e. $s'(f_n) = .25\, s(f_{n-1}) + 0.50\, s(f_n) + 0.25\, s(f_{n+1})$ shows one set of weights commonly used. These weights are called the "Hanning"

weights after the man who first used them. The method is also adapted for calculating the statistical significance of the spectral estimates.

Now that the fast Fourier transform technique of Cooley and Tukey (1965) has made it computationally advantageous to compute spectra directly without an intermediate calculation of an autocovariance function, another method of smoothing is desirable. Welch (1967) suggests obtaining spectral estimates from several intervals and averaging. He describes multiplying the data by weights before obtaining the spectral estimates rather than multiplying the spectral estimates by smoothing weights later. The method is applicable to the fast Fourier transform techniques, and like the autocovariance method, it permits calculation of the statistical significance of the spectral estimates.

If the data contains a strong repetitive cycle, such as the whale calls studied by Singleton and Poulter (1967), the spectrum will contain a sharp peak, and another problem can arise. If the frequency of the repetitive cycle falls <u>between</u> two of the calculated points for the spectrum, these two points and all the rest of the calculated points will be affected. As explained by Bingham et al. (1967), the effects of the peak have alternating signs and decay slowly (like $\frac{1}{|f-f_n|}$) as f_n recedes from the peak frequency, f. Before computation of the spectral density from Equation A.2.34, they recommend that the Fourier coefficients be hanned according to

$$S'(f_n) = 0.25S(f_{n-1}) + 0.50S(f_n) + 0.25S(f_{n+1})$$

when the time origin is in the center of the data or according to

$$S'(f_n) = -0.25S(f_{n-1}) + 0.50S(f_n) - 0.25S(f_{n+1})$$

when the time origin is at the first data point. The hanning causes the effect of a peak to decay like $\frac{1}{|f-f_n|^3}$ so that the resulting calculated spectrum will have a sharper peak more like the true underlying spectrum.

An alternate procedure is discussed by Blackman and Tukey (1959). In cases like that discussed in the preceding paragraph, where a strong repetitive cycle causes a rapid change of spectral density with frequency, they suggest that the data be adjusted prior to the computation of the spectrum in a way which will make the spectrum more flat. Such an adjustment is called <u>prewhitening</u> because the spectrum is made to resemble more closely the flat spectrum of "white" noise which has equal spectral density for all frequencies. The prewhitening adjustment may be accomplished by

$$p'(t_k) = p(t_k) - a\, p(t_{k-1})$$

Where

$p'(t_k)$ = the adjusted value of p

and a = a constant ≤ 1. (Blackman and Tukey use $a = 0.6$ in one of their examples.) However, prewhitening by this means introduces a phase change in the data which may be undesirable if any cross spectral analysis (soon to be discussed) is performed.

6. Aliasing

If frequencies higher than $\frac{1}{(2\Delta t)}$ were originally present in p, they will unfortunately "alias" the digital data when it is sampled at discrete points, as illustrated in Figure A.2.9 and explained by Blackman and Tukey (1958). The solid line in the figure denotes a harmonic whose frequency is higher than $\frac{1}{(2\Delta t)}$. When the sampling is performed at the Δt intervals,

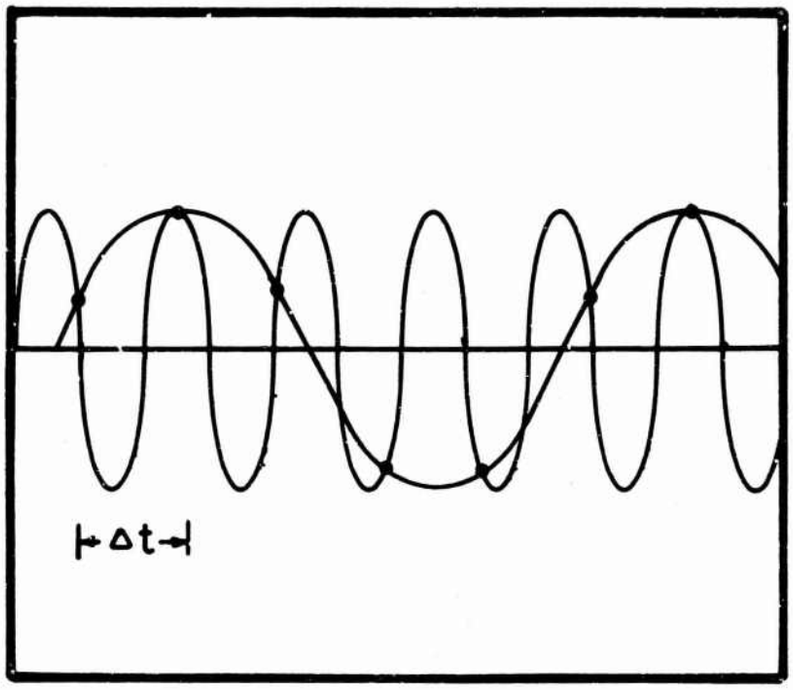

Figure A.2.9 Illustration of how digital sampling may cause a high frequency component to alias and appear as a low frequency component

the variability in p due to this higher frequency component appears instead to be the lower frequency harmonic shown by the dashed line. Hence, the lower frequency harmonics will appear larger than they are in reality if some of the variability in p is due to harmonics of frequency higher than $\frac{1}{(2\Delta t)}$. In the practical situation, then, one must make Δt small enough so that all important frequencies can be considered, and must filter out any higher frequency "noise" before the data is sampled. Filtering can be accomplished by using special electrical filters ahead of the recording equipment or by using recording equipment which has a long mechanical time constant.

7. Trends

If the data show a general tendency to increase or decrease over the total sampling period, T, they are said to contain a trend. The presence of a trend means that a portion of the variance is due to frequencies lower than the lowest distinguishable frequency, 1/T. When the spectrum is computed, the spectral density at the low frequency end will be artificially high with the point for frequency 1/T being affected most. The usual method for correction is to remove the trend from the data before the calculation of the spectrum. The equation of the trend line can be computed from the data by the method of least squares; then the corresponding trend values can be subtracted from each data point.

III. CROSS-SPECTRAL ANALYSIS

Spectral analysis may also be used to study phase and amplitude relationships between the fluctuations of two entities, p_1 and p_2.

Consider the Fourier transforms, as defined by Equation A.2.30, of the data from <u>two</u> time series. Presume also that the data have zero mean or have had the mean subtracted from each of the data points. Thus,

$$S_1(-f_n) = \Delta t \sum_{j=-\frac{(N-1)}{2}}^{\frac{N-1}{2}} p_1(t_j) \exp(i2\pi f_n t_j) \qquad \text{A.3.1}$$

$$S_2(f_n) = \Delta t \sum_{j=-\frac{(N-1)}{2}}^{\frac{N-1}{2}} p_2(t_j) \exp(-i2\pi f_n t_j) \qquad \text{A.3.2}$$

$$n = -\frac{(N-1)}{2}, \ldots\ldots, -1, 0, 1, \ldots\ldots \frac{N-1}{2}$$

If one computes $\Delta f\, S_1(-f_n)\, S_2(f_n)$ analogous to Equation A.2.34, a spectral density function is obtained, but it is quite different from the spectral density function of Equation A.2.34. Because $S_2(f_n)$ is not the complex conjugate of $S_1(-f_n)$, the new spectral density function has both real and imaginary parts. It is called the <u>cross spectral density function</u> and will here be denoted $s_c(f_n)$.

$$s_c(f_n) = \Delta f\, S_1(-f_n)\, S_2(f_n) \qquad \text{A.3.3}$$

That $s_c(f_n)$ has both real and imaginary parts may be illustrated by the following. Let

$$S_1(-f_n) = a_n + ib_n \qquad \text{A.3.4}$$

and $$S_2(f_n) = c_n - id_n \qquad \text{A.3.5}$$

where a_n, c_n, and b_n, d_n, are real and imaginary parts, respectively, of $S_1(f_n)$ and $S_2(f_n)$. Then, using Equations A.3.4 and A.3.5 in A.3.3,

$$s_c(f_n) = f(a_n c_n + b_n d_n) + i\ f(b_n c_n - a_n d_n) \qquad \text{A.3.6}$$

In general, $b_n c_n \neq a_n d_n$, because the $S_1(f_n)$ and $S_2(f_n)$ are from two different time series, and so $s_c(f_n)$ is complex.

A complex number may also be written in the form of an amplitude times a phase factor, so that

$$S_1(-f_n) = A_{1n}\exp(i\phi_{1n}) \qquad \text{A.3.7}$$

and $$S_2(f_n) = A_{2n}\exp(-i\phi_{2n}) \qquad \text{A.3.8}$$

where

$$A_{1n} = \sqrt{a_n^2 + b_n^2}$$

$$\phi_{1n} = \arctan \frac{b_n}{a_n}$$

$$A_{2n} = \sqrt{c_n^2 + b_n^2}$$

$$\phi_{2n} = \arctan \frac{d_n}{c_n}$$

These forms will soon be useful. Equation A.3.6 may be written

$$s_c(f_n) = C(f_n) - iQ(f_n) \qquad \text{A.3.9}$$

The real part, $C(f_n)$, is called the <u>co-spectrum</u>. The imaginary part, $Q(f_n)$, is called the <u>quadrature</u> spectrum. If, in Equation A.3.6, $b_n c_n = a_n d_n$, then $\phi_{1n} = \phi_{2n}$, and the two times series are <u>in-phase</u>. Also, then

$Q(f_n) = 0$, so $s_c(f_n) = C(f_n)$, and thus, $C(f_n)$ is also called the <u>in-phase spectrum</u>. Recall from Equation A.2.26 that $s(f_n)$ represents the variance in p per frequency increment. Analogously, $C(f_n)$ represents the cross-covariance between p_1 and p_2 per frequency increment for various frequencies when the two series are in-phase. If, in Equation A.3.6 $a_n c_n = -b_n d_n$, then $\phi_{1n} = \phi_{2n} + \pi/2$ and the two time series are out-of-phase. Then $C(f_n) = 0$, so $s_c(f_n) = -i\ Q(f_n)$, and $Q(f_n)$ is also called the <u>out-of-phase spectrum</u>. $Q(f_n)$ represents the cross-covariance between p_1 and p_2 per frequency increment for various frequencies when one of the series is shifted exactly 1/4 period with respect to the other.

The degree of phase shift between the two time series for various frequencies is measured by the <u>phase spectrum</u>, defined by

$$\phi(f_n) = \arctan \frac{Q(f_n)}{C(f_n)} \qquad \text{A.3.10}$$

To measure the degree of similarity of amplitude between the two time series for various frequencies, a <u>cross-amplitude spectrum</u> is defined by

$$A(f_n) = \sqrt{[C(f_n)]^2 + [Q(f_n)]^2} \qquad \text{A.3.11}$$

$A(f_n)$ is usually normalized and used in the form

$$\text{Coh}\ (f_n) = \frac{C(f_n)^2 + Q(f_n)^2}{s_1(f_n)\ s_2\ (f_n)} \qquad \text{A.3.12}$$

$\text{Coh}(f_n)$ is called the <u>coherence</u> and measures how well the two time series are correlated for various frequencies. As explained by Panofsky and Brier (1965), the coherence varies from 0 to 1 and is analogous to the square of a correlation coefficient. Probability tables have been

established for coherence functions which have been computed from transforms of cross covariance function, soon to be defined. The tables can be used to test the closeness of the relationship between the two series at the various frequencies.

However, if one writes out $Coh(f_n)$ explicitly in terms of raw Fourier coefficients, one obtains

$$Coh(f_n) = \frac{[\Delta f(a_n c_n + b_n d_n)]^2 + [\Delta f(b_n c_n - a_n d_n)]^2}{(\Delta f)\ (a_n - ib_n)(a_n + ib_n)(\Delta f)(c_n + id_n)(c_n - id_n)} = 1 \qquad \text{A.3.13}$$

for every frequency f_n. Although Equation A.3.13 may seem rather surprising after the comments in the preceding paragraph, the explanation is rather simple. When computed from raw coefficients, Equation A.3.12 is the same as a correlation coefficient computed from one observation pair. Therefore, the coherence must be computed from coefficients which have been smoothed or averaged in some way. The current practice is to form a weighted average over several frequencies of each quantity in Equation A.3.12, but, as discussed by Tick (1967), the best method to do the smoothing and its corresponding table of confidence limits have not yet been satisfactorily established.

In Fig. A.3.1 are plotted the coherence and the phase spectrum for air pressure between a point on the ground surface in a field and another point downwind from the first. For low frequencies, the pressure is the same at the two points, so the coherence is close to one and the phase angle between them is close to zero. As frequency increases, the corresponding wave lengths of pressure waves moving across the field become smaller. The pressure at the upwind point changes before that at the downwind point

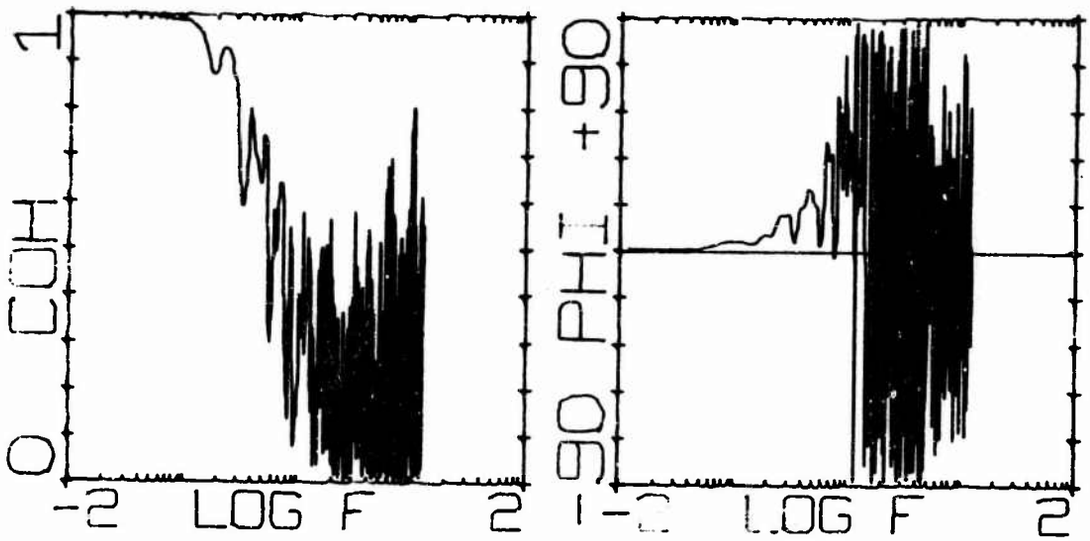

Figure A.3.1 Coherence and phase spectrum for air pressure between a point on the ground surface in a field and another point downwind from the first

and is shown in the figure by an increasing phase angle between the points with increasing frequency. As frequency becomes higher (and wave length smaller), the two points do not always see the same wave, as evidenced by the decrease in coherence with frequency. When the coherence gets small, the phase angle changes wildly and is no longer meaningful.

If the convolution procedure is performed on $S_1(-f_n)S_2(f_n)$ exactly as it was on $S(-f_n)S(f_n)$ in Equations A.2.39 through A.2.42, one finds that

$$R_c(\tau_u) = \frac{1}{N-1} \sum_{j=-\frac{(N-1)}{2}}^{\frac{N-1}{2}} p_1(t_j)\, p_2(t_j + \tau_u), \qquad \text{A.3.14}$$

$$R_c\,(\tau_u) = \Delta f \sum_{n=\frac{-(N-1)}{2}}^{\frac{N-1}{2}} s_c(f_n)\, \exp(i2\pi f_n \tau_u)\ , \qquad \text{A.3.15}$$

and

$$s_c(f_n) = \Delta t \sum_{u=\frac{-(N-1)}{2}}^{\frac{N-1}{2}} R_c(\tau_u)\, \exp(-i2\pi f_n \tau_u) \qquad \text{A.3.16}$$

where $R_c(\tau_u)$ is the <u>cross-covariance function</u> and τ_u is a lag in time by which one time series is shifted with respect to the other. When $\tau_u = 0$, $R_c(\tau_u)$ is identically equal to the usual covariance from elementary statistics, i.e.

$$R_c(0) = \frac{1}{N-1} \sum_j p_1(t_j)\, p_2(t_j) \qquad \text{A.3.17}$$

If one describes both p_1 and p_2 in Equation A.3.17 by a Fourier series, one obtains an equation analogous to Equation A.2.17. Proceeding similarly to the steps in Section A.II.2 and Section A.II.3, one finds that the contributions of the various harmonics to the covariance may be

evaluated and plotted to form a spectrum. The spectrum is identical to the cospectrum, and the area under the curve is equal to the covariance. The latter fact can be used to evaluate the covariance, and has been used, for instance, by McBean (1968) to obtain the covariance between temperature and vertical wind (in this case, the covariance was particularly useful because it is equal to the vertical eddy flux of heat.)

If Equation A.3.15 is used for its computation, the cross-covariance function obtained will be a circular cross-covariance whereby the overlapping values at the ends of the time series due to the offset lag τ_u are shifted around to the front. If Equation A.3.14 is used for its computation, the summing and averaging are usually performed only over pairs of values which do not overlap. One notes from Equations A.3.15 and A.3.16 that the cross spectral density function and the cross-covariance function are Fourier transforms of one another.

IV. TWO-DIMENSIONAL SPECTRAL ANALYSIS

Some entities fluctuate with respect to more variables than just time. In this section, the concepts introduced for one-dimensional spectral analysis are expanded to two dimensions. Although the orientation taken here is for one of the dimensions to be time and for the other to be distance parallel to the wind, the concepts apply as well to any two variables. Just as it will be shown how to extend the concepts from one to two variables, the concepts can also be expanded to include more than two variables. Lumley and Panofsky (1964), for example, discuss spectra of entities that fluctuate with four variables, time and space in three directions.

1. Fourier series representation

Suppose p represents a variable such as pressure in some turbulent field moving horizontally over the ground surface, so that $p = p(t, x)$ where t it time and x is the horizontal distance. One observes the pressure N times at each of M positions in the turbulent field. At each position the observations are taken starting at $t = -\frac{T}{2}$ for a total period of time T. The observations are spaced Δt units apart, and the time at which each is taken is $t_j = j\Delta t$ for $j = \frac{-(N-1)}{2}, \ldots$ $1, 0, 1, \ldots \frac{N-1}{2}$. We note that $T = (N-1)\Delta t$. The observation positions are spaced along a line parallel to the direction of movement of the field. The total length covered is L, and the first position is at $x = -\frac{L}{2}$. The positions are spaced x units apart, and an individual position is denoted by $x_\ell = \ell\Delta x$ for $\ell = \frac{-(N-1)}{2}, \ldots, -1, 0, 1, \ldots \frac{N-1}{2}$. We note that $L = (M-1)\Delta x$. The notation is illustrated in Figure A.4.1 where the vertical direction out of the paper represents the magnitude of p.

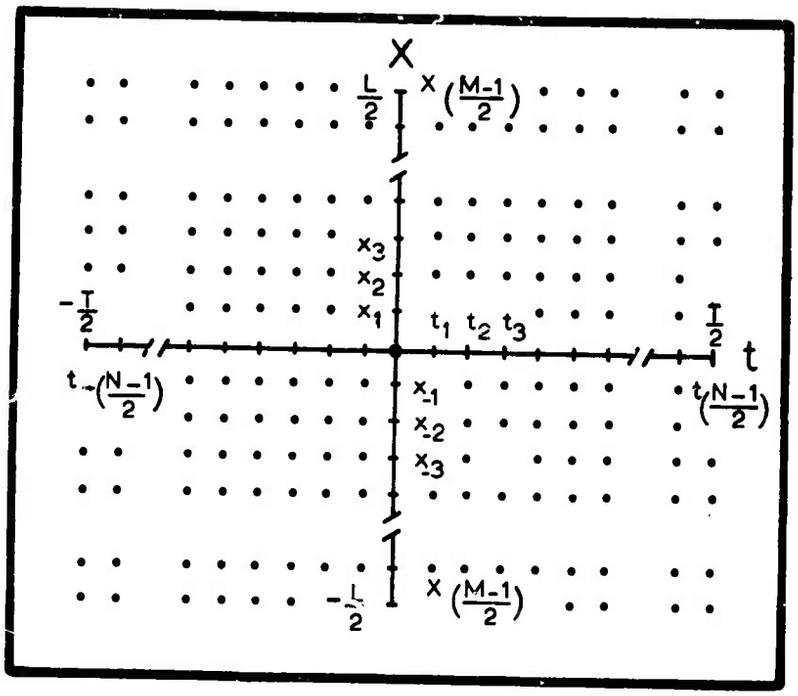

Figure A.4.1 Illustration of coordinate system and notation for sampling p

Analogous to the one-dimensional case, p can be represented by a Fourier series of complex exponentials. The two-dimensional forms of Equations A.2.1, A.2.2, and A.2.3 are:

$$p(t, x) = \sum_{n=-\infty}^{\infty} \sum_{m=-\infty}^{\infty} C_{n,m} \exp[i2\pi(\frac{nt}{T} - \frac{mx}{L})] \qquad \text{A.4.1}$$

$$\int_{-T/2}^{T/2} \int_{-L/2}^{L/2} \exp[i2\pi(\frac{nt}{T} - \frac{mx}{L})] \exp[i2\pi(\frac{qt}{T} - \frac{rx}{L})]\, dt = TL \text{ when } q = -n \text{ and } r = -m$$

$$= 0 \quad \text{for all other cases} \qquad \text{A.4.2}$$

$$C_{n,m} = \frac{1}{TL} \int_{-T/2}^{T/2} \int_{-L/2}^{L/2} p(t,x) \exp[i2\pi(\frac{nt}{T} - \frac{mx}{L})]\, dt \qquad \text{A.4.3}$$

And, analogously to the one-dimensional case, Equations A.4.1 and A.4.3 are discretized to conform to the discrete data. Equation A.4.1 becomes

$$p(t_j, x_\ell) = \sum_{n=-\frac{(N-1)}{2}}^{\frac{N-1}{2}} \sum_{m=-\frac{(M-1)}{2}}^{\frac{M-1}{2}} C_{n,m} \exp[i2\pi(\frac{nt_j}{T} - \frac{mx_\ell}{L})] \qquad \text{A.4.4}$$

Equation A.4.3 becomes

$$C_{n,m} = \frac{\Delta t \Delta x}{TL} \sum_{j=-\frac{(N-1)}{2}}^{\frac{N-1}{2}} \sum_{\ell=-\frac{(N-1)}{2}}^{\frac{N-1}{2}} p(t_j, x_\ell) \exp[-i2\pi(\frac{nt_j}{T} - \frac{mx_\ell}{L})] \qquad \text{A.4.5}$$

As in the one dimensional case, the terms corresponding to n and -n represent harmonics or frequencies. However, now we have the additional

complication of an added dimension; the m, -m pairs represent cycles per total length L or wave numbers.

2. Relation of variance to spectral density function

The variance for p, which is a function of two variables, may be written as

$$s^2 = \frac{1}{MN-1} \sum_{j=-\frac{(N-1)}{2}}^{\frac{N-1}{2}} \sum_{\ell=-\frac{(N-1)}{2}}^{\frac{N-1}{2}} [p(t_j, x_\ell) - \bar{p}]^2 \qquad \text{A.4.6}$$

where the $\bar{p}$ is the mean of all NM observations.

Note in Equation A.4.4 that the mean $C_{o,o}$ assuming MN >> 1, substitution of Equation A.4.4 into A.4.6 yields

$$s^2 = \frac{\Delta t \Delta x}{TL} \sum_j \sum_\ell [\sum_n \sum_m C_{n,m} \exp[i2\pi(\frac{nt_j}{T} - \frac{mx_\ell}{L})] - C_{o,o}]^2 \qquad \text{A.4.7}$$

Equation A.4.7 is the numerical integration form for

$$s^2 = \frac{1}{TL} \int_{-T/2}^{T/2} \int_{-L/2}^{L/2} [\sum_n \sum_m C_{n,m} \exp[i2\pi(\frac{nt_j}{T} - \frac{mx}{L})] - C_{o,o}]^2 \, dt \, dx \qquad \text{A.4.8}$$

Analogous to the one-dimensional case, if the long series above is written out, squared, and integrated, all terms will equal zero except those whose coefficients are $C_{-n,-m} C_{n,m}$ or $C_{-n,m} C_{n,-m}$. Thus, carrying out the above operations with the aid of Equation A.4.2

$$s^2 = \sum_{n=\frac{-(N-1)}{2}}^{\frac{N-1}{2}} \sum_{m=\frac{-(M-1)}{2}}^{\frac{M-1}{2}} C_{n,m} C_{-n,-m} - C_{o,o}^2$$

$$= \sum_{n=\frac{-(N-1)}{2}}^{\frac{N-1}{2}} \sum_{m=\frac{(M-1)}{2}}^{\frac{M-1}{2}} |C_{n,m}|^2 - C_{o,o}^{\ 2} \qquad \text{A.4.9}$$

where the vertical bars denote modulus. The squared modulus results because, analogous to the one-dimensional case, the $C_{-n,-m}$ and $C_{n,m}$ are complex conjugates.

The term corresponding to each n,m pair represents the contribution of the n/T th frequency and m/L th wave number to the total variance. If we now define

$$f_n = n/T \qquad \text{A.4.10}$$

$$\Delta f = 1/T \qquad \text{A.4.11}$$

$$k_m = m/L \qquad \text{A.4.12}$$

and $\Delta k = 1/L$ and plot A.4.13

$|C_{n,m}|^2$ against f_n and k_m, we obtain a Fourier line spectrum. In Figure A.4.2 each dot represents a certain value of $|C_{n,m}|^2$ extending in a line up out of the paper.

If the $|C_{n,m}|^2$ are distributed uniformly over the rectangle f_{n-1} to f_n and k_{m-1} to k_m, one obtains a three-dimensional histogram where the height of the rectangular parallelpipeds can be obtained from

$$|C_{n,m}|^2 = (\text{height})\ (\Delta k)\ (\Delta f) \qquad \text{A.4.14}$$

or

$$\text{height} = \frac{1}{\Delta k \Delta f}\ |C_{n,m}|^2 \qquad \text{A.4.15}$$

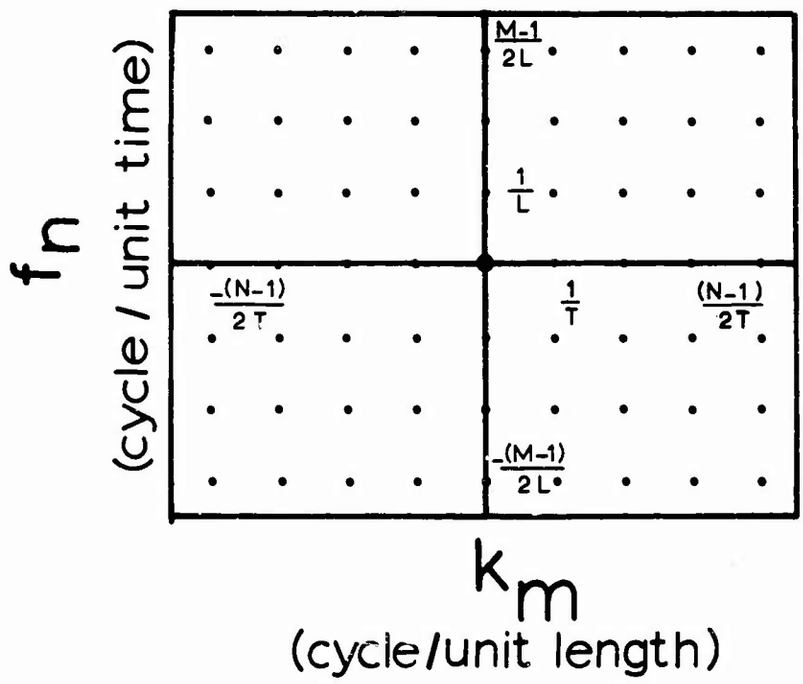

Figure A.4.2 Plot of Fourier line spectrum

Figure A.4.3 illustrates the 3 dimensional "periodogram." The height of the rectangular parallelpipeds is $\frac{1}{\Delta k \Delta f} |C_{n,m}|^2$ and extends up out of the paper.

As $T \to \infty$ and $L \to \infty$ more and more values of $\frac{1}{\Delta f \Delta k}$ are obtained, the "periodogram" becomes a continuous surface. The smooth continuous surface, called here $s(f_n, k_m)$ is the two-dimensional <u>spectral density function</u>. It is shown plotted by contour lines of constant spectral density in Figure A.4.4. Figure A.4.4 is a two-dimensional power spectrum or variance spectrum where

$$s(f_n, k_m) = \frac{1}{\Delta f \Delta k} |C_{n,m}|^2$$

$$n = \frac{-(N-1)}{2}, \ldots\ldots -1, 0, +1, \ldots \frac{N-1}{1}$$

$$m = \frac{-(M-1)}{2}, \ldots\ldots -1, 0, +1, \ldots \frac{M-1}{2} \qquad \text{A.4.16}$$

The two-dimensional spectral density function represents the variance in p per increment of frequency and wave number. The total volume under the surface represents the total variance. The graph can be normalized, if desired, by dividing $s(f_n, k_m)$ by the total variance calculated directly from Equation A.4.6. The normalized graph will always have the volume under the graph equal to one.

The point where $n = m = 0$ is equal to $\bar{p}^2$ and represents the variance at zero wave number and zero frequency. From Equation A.4.9, however, note that it is not included in the summation for the total variance.

Since a wave with a positive f_n and positive k_m and a wave with a negative f_n and a negative k_m are identical waves traveling in the positive

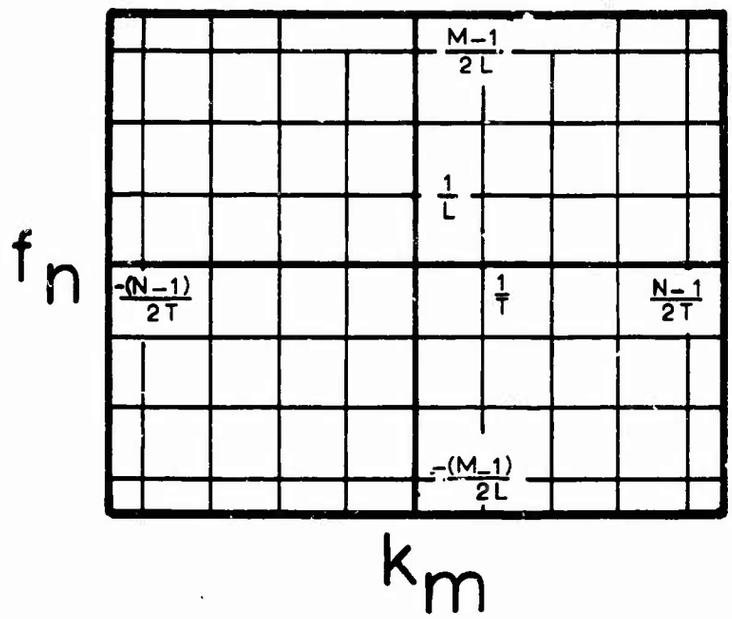

Figure A.4.3 Plot of 3-D "periodogram"

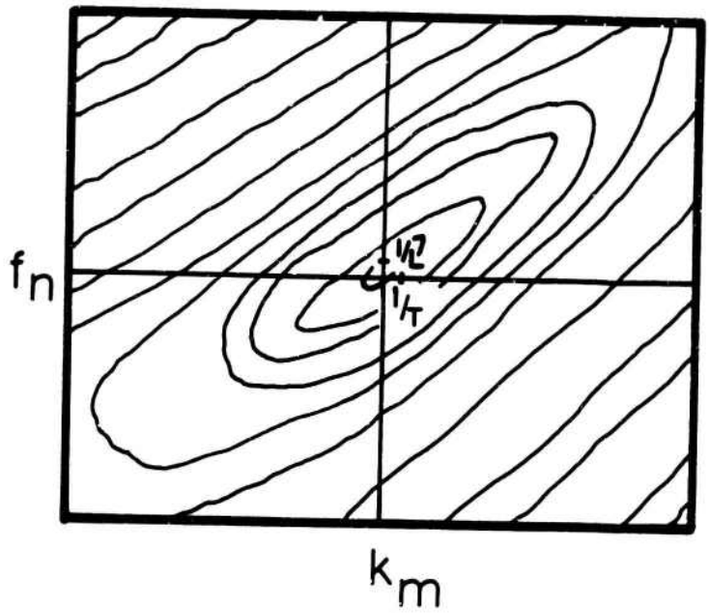

Figure A.4.4 Contour surface of spectral density function, $s(f_n, k_m)$, plotted against frequency and wave number

x direction, the wave with negative f_n and k_m may be ignored if the amplitude of the other wave is multiplied by two. Also, since a wave with a positive f_n and negative k_m and a wave with a negative f_n and positive k_m are identical waves traveling in the negative x direction, the wave with the positive f_n and negative k_m may be ignored if the amplitude of the other wave is multiplied by two.

One may take advantage of the preceding two statements by defining wave numbers to be positive quantities only and by regarding frequencies to be both positive and negative.

The decision to define wave numbers as only positive quantities causes changes in Equations A.4.9, A.4.14, A.4.15, and A.4.16.

Equation A.4.9 becomes

$$s^2 = 2 \sum_{n=\frac{-(N-1)}{2}}^{\frac{N-1}{2}} \sum_{m=0}^{\frac{M-1}{2}} |C_{n,m}|^2 - 2 \sum_{n=0}^{\frac{N-1}{2}} |C_{n,0}|^2 \qquad \text{A.4.17}$$

and Equation A.4.16 becomes

$$s(f_n,k_m) = \frac{2}{\Delta f \Delta k} |C_{n,m}|^2$$

$$r = \frac{-(N-1)}{2}, \ldots\ldots, -1, 0, 1, \ldots\ldots \frac{N-1}{2} \qquad \text{A.4.18}$$

$$m = 0, 1, 2, \ldots\ldots\ldots\ldots\ldots\ldots \frac{M-1}{2}$$

3. Relation of two-dimensional spectral density function to Fourier transform.

In manipulations exactly analogous to the one-dimensional case, we can form a discrete two-dimensional Fourier transform pair by substituting

the expressions from $C_{n,m}$ given by Equation A.4.4 into Equation A.4.4. One then defines

$$S(f_n,k_m) = \Delta t \Delta x \sum_j \sum_\ell p(t_j,x_\ell) \exp[-i2\pi(t_j f_n - x_\ell k_m)] \qquad \text{A.4.19}$$

and then

$$p(t_j,x_\ell) = \Delta f \Delta k \sum_n \sum_m S(f_n,k_m) \exp[i2\pi(t_j f_n - x_\ell k_m)] \qquad \text{A.4.20}$$

Equations A.4.19 and A.4.20 form the transform pair. Analogous to Equation A.2.32 one obtains

$$S(f_n,k_m) = \frac{C_{n,m}}{\Delta f \Delta k} \qquad \text{A.4.21}$$

and also since $C_{-n,-m}$ and $C_{n,m}$ are complex conjugates,

$$s(f_n,k_m) = \Delta f \Delta k \, |S(f_n,k_m)|^2$$

$$n = \frac{-(N-1)}{2}, \ldots\ldots, -2, -1, 0, 1, 2, \ldots\ldots \frac{N-1}{2} \qquad \text{A.4.22}$$

$$m = \frac{-(M-1)}{2}, \ldots\ldots, -2, -1, 0, 1, 2, \ldots\ldots \frac{M-1}{2}$$

Thus, the spectral density surface may be computed by a double Fourier transform of the data for $n = \frac{-(N-1)}{2}, \ldots -2, -1, 0, 1, 2 \ldots \frac{N-1}{2}$ and $m = \frac{-(M-1)}{2}, \ldots\ldots -2, -1, 0, 1, 2 \ldots \frac{M-1}{2}$, and then multiplying each of the $S(f_n,k_m)$ by its complex conjugate times $\Delta f \Delta k$.

The computation of $S(f_n,k_m)$ may be carried out using the fast Fourier transform described by Brigham and Morrow (1967). To illustrate, let Equation A.4.19 be written as:

$$S(f_n,k_m) = \Delta t \sum_j [\Delta x \sum_\ell p(t_j,x_\ell) \exp(i2\pi x_\ell k_m)] \exp(-i2\pi t_j f_n) \qquad \text{A.4.23}$$

The quantity in brackets, denote it $S(t_j,k_m)$ is simply the one-dimensional Fourier transform of the data. It is the same as Equation A.2.30 except the transformation is with respect to wave number instead of frequency. Thus, using the fast Fourier transform, one calculates

$$S(t_j,k_m) = \Delta x \sum_{\ell} p(t_j,x_\ell) \exp(i2\pi x_\ell k_m) \qquad \text{A.4.24}$$

Then applying the transform a second time, one calculates,

$$S(f_n,k_m) = \Delta t \sum_{j} S(t_j,k_m) \exp(-i2\pi k_j f_n) \qquad \text{A.4.25}$$

The above process may also be used to calculate $p(t_j,x_\ell)$ from $S(f_n,k_m)$ in Equation A.4.20.

4. Relation of two-dimensional spectral density function to two-dimensional covariance function.

The two-dimensional autocovariance function is defined

$$R(\tau_u,\delta_v) = \frac{1}{(N-u)\ (M-v) - 1} \sum_{j = \frac{-(N-1-u)}{2}}^{\frac{N-1-u}{2}} \sum_{\ell = \frac{-(M-1-u)}{2}}^{\frac{M-1-v}{2}} [p(t_j,x_\ell)-\bar{p}]$$

$$[p(t_j + \tau_u,\ x_\ell + \delta_v)-\bar{p}] \qquad \text{A.4.26}$$

where the bar denotes the mean. τ_u represents a lag in time, and it is usually an integer multiple of Δt, i.e., $\tau_u = u\Delta t$ where u is an integer. δ_v represents a spacing between observation stations, and it usually is an integer multiple of Δx, i.e. $\delta_v = v\Delta x$, where v is an integer.

When $N >> u$, $M >> v$, and $\bar{p} = 0$ (the mean can be subtracted from all points if necessary), Equation A.4.26 becomes

$$R(\tau_u,\delta_v) = \frac{1}{NM} \sum_{u=\frac{-(N-1)}{2}}^{\frac{N-1}{2}} \sum_{v=\frac{-(M-1)}{2}}^{\frac{M-1}{2}} p(t_j, x_\ell)\, p(t_j + \tau_u, x_\ell + \delta_v) \qquad \text{A.4.27}$$

A convolution procedure analogous to the one-dimensional case reveals the two-dimensional autocovariance function to be the double Fourier transform of the two-dimensional spectral density function so that

$$R(\tau_u,\delta_v) = \Delta f \Delta k \sum_{n=\frac{-(N-1)}{2}}^{\frac{N-1}{2}} \sum_{m=\frac{-(M-1)}{2}}^{\frac{M-1}{2}} s(f_n,k_m) \exp[i2\pi(f_n\tau_u - k_m\delta_v)] \qquad \text{A.4.28}$$

The spectral density function must also be the double Fourier transform of the autocovariance function or

$$s(f_n,k_m) = \Delta t \Delta x \sum_{u=\frac{-(N-1)}{2}}^{\frac{N-1}{2}} \sum_{v=\frac{-(M-1)}{2}}^{\frac{M-1}{2}} R(\tau_u,\delta_v) \exp[-i2\pi(f_n\tau_u - k_m\delta_v)] \qquad \text{A.4.29}$$

The autocovariance function in Equation A.4.28 is not the usual autocovariance function but a circular autocovariance function where the overlapping values at the ends of the summation intervals in the usual autocovariance function, Equation A.4.28, have been shifted to the fronts. This is why u goes from $\frac{-(N-1)}{2}$ to $\frac{N-1}{2}$ and v from $\frac{-(M-1)}{2}$ to $\frac{M-1}{2}$ in Equations A.4.28 and A.4.29 even though the assumption was stated that $N >> u$ and $M >> v$ in going from Equation A.4.26 to Equation A.4.27.

It can be deduced from Equation A.4.27 that $R(\tau_u,\delta_u) = R(-\tau_u,-\delta_v)$ and that $R(-\tau_u,\delta_v) = R(\tau_u,-\delta_v)$. Thus, Equation A.4.29 may be modified to include only positive spacings so that

$$s(f_n,k_m) = 2\Delta t\Delta x \sum_{u=\frac{-(N-1)}{2}}^{\frac{N-1}{2}} \sum_{v=0}^{\frac{M-1}{2}} R(\tau_u,\delta_v) \exp[-i2\pi(f_n\tau_u - k_m\delta_v)] \qquad \text{A.4.30}$$

From Equation A.4.18 it can also be seen that Equation A.4.28 may be modified to include only positive wave numbers so that

$$R(\tau_u,\delta_v) = 2\Delta f\Delta k \sum_{n=\frac{-(N-1)}{2}}^{\frac{N-1}{2}} \sum_{m=0}^{\frac{M-1}{2}} s(f_n,k_m) \exp[i2\pi(f_n\tau_u - k_m\delta_v)]$$

V. USE OF CROSS SPECTRAL DENSITY FUNCTIONS IN TWO-DIMENSIONAL ANALYSIS

To calculate the two-dimensional spectral density function from Equations A.4.19 and A.4.22, N observations are required at each of M observation stations. Since N and M are both usually very large numbers, it is desirable to have methods which require less acquisition and processing of data. Under certain assumptions, discussed in this section, it is possible to calculate the two-dimensional spectral density function from data taken at drastically fewer than M stations. The orientation is again toward an entity which fluctuates with time and one direction in space, but the methods can be applied wherever the assumptions are valid.

1. The assumptions of stationarity and spacial homogeneity

Suppose p is observed with time at several points separated by a spacing $\delta_v = v\Delta x$ units of distance from some space origin. The sampling scheme is illustrated in Figure A.5.1. One subtracts the mean from all observations so that only the fluctuations in p are considered.

When p is statistically stationary, the mean, the variance, and other statistical parameters of p do not change with time even though p itself is fluctuating constantly. If p is spacially homogeneous, the mean, the variance, and other statistical parameters do not change with distance. When one can assume that p is statistically stationary and spacially homogenous, the two-dimensional autocovariance function

$$R(\tau_u,\delta_v) = \frac{1}{NM} \sum_{j=\frac{-(N-1)}{2}}^{\frac{N-1}{2}} \sum_{\ell=\frac{-(M-1)}{2}}^{\frac{M-1}{2}} p(t_j,x_\ell)p(t_j+\tau_u, x_\ell+\delta_u) \qquad \text{A.5.1}$$

is a function only of the time and space increments τ_u and δ_v. It does not change with a new origin of time or a new origin of space.

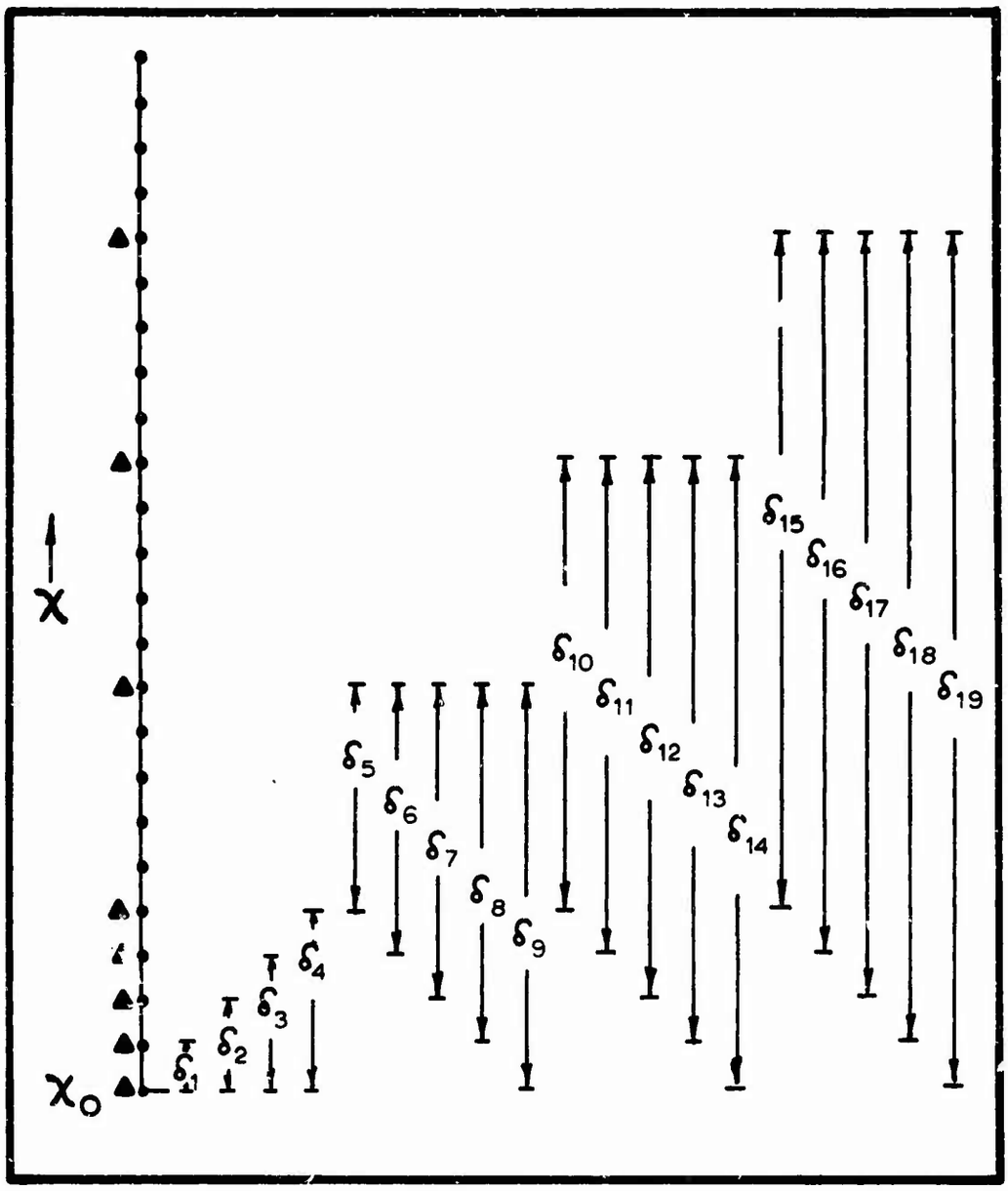

Figure A.5.1 Sampling scheme which can be used where p is statistically stationary and spacially homogeneous

Equation A.5.1 can be written

$$R(\tau_u,\delta_v) = \frac{1}{M} \left\{ \frac{1}{N} \sum_{j=\frac{-(N-1)}{2}}^{\frac{N-1}{2}} p(t_j, x_{\frac{-(N-1)}{2}})\, p(t_j + \tau_u,\, x_{\frac{-(N-1)}{2}} + \delta_v) \right.$$

$$+ \cdots\cdots$$

$$+ \cdots\cdots$$

$$+ \cdots\cdots$$

$$+ \frac{1}{N} \sum_{j=\frac{-(N-1)}{2}}^{\frac{N-1}{2}} p(t_j, x_o)\, p(t_j + \tau_u,\, x_o + \delta_v)$$

$$+ \cdots\cdots$$
$$+ \cdots\cdots$$
$$+ \cdots\cdots$$
$$+ \cdots\cdots$$
$$+ \cdots\cdots$$

$$\left. + \frac{1}{N} \sum_{j=\frac{-(N-1)}{2}}^{\frac{N-1}{2}} p(t_j, x_{\frac{N-1}{2}})\, p(t_j + \tau_u,\, x_{\frac{N-1}{2}} + \delta_v) \right\} \qquad \text{A.5.2}$$

and one notes that under the above assumption, all of the sums on j are equal. Since there are M of the sums,

$$R(\tau_u,\delta_v) = \frac{1}{N} \sum_{j=\frac{-(N-1)}{2}}^{\frac{N-1}{2}} p(t_j, x_o)\, p(t_j + \tau_u,\, x_o + \delta_v) \qquad \text{A.5.3}$$

Recalling Equation A.3.14 one sees that $R(\tau_u,\delta_v)$ is equal to the cross covariance, $R_c(\tau_u,\delta_v)$, between the pressure at point x_o and point $x_o + \delta_v$. Thus,

$$R(\tau_u,\delta_v) = R_c(\tau_u,\delta_v) \qquad \text{A.5.4}$$

which is an important simplification and can drastically reduce the required number of measurements where the assumptions are valid.

2. Relationship between cross spectral density function and 2-D spectral density function.

The Fourier transforms of the data gathered by the scheme in Figure A.5.1 can be computed for each of the sampling points according to Equation A.2.30 which is rewritten here.

$$S(-f_n,x_o) = \Delta t \sum_{j=\frac{-(N-1)}{2}}^{\frac{N-1}{2}} p(t_j,x_o)\exp(i2\pi f_n t_j) \qquad \text{A.5.5}$$

$$S(f_n, x_o + \delta_v) = \Delta t \sum_{j=\frac{-(N-1)}{2}}^{\frac{N-1}{2}} p(t_j, x_o + \delta_v)\exp(-i2\pi f_n t_j) \qquad \text{A.5.6}$$

The cross spectral density function between the two points, recalling Equation A.3.3, is

$$s_c(f_n,\delta_v) = \Delta f \;\; S(-f_n,x_o)S(f_n, x_o + \delta_v) \qquad \text{A.5.7}$$

By Equation A.3.16, it is also equal to the Fourier transform of the cross-covariance function

$$s_c(f_n,\delta_v) = \Delta t \sum_{u=\frac{-(N-1)}{2}}^{\frac{N-1}{2}} R_c(\tau_u,\delta_v)\exp(i2\pi f_n \tau_u) \qquad \text{A.5.8}$$

Now, suppose one computes a two-dimensional spectrum, called here $W(f_n,k_m)$, by a Fourier transform of $s_c(f_n,\delta_v)$ according to:

$$W(f_n,k_m) = \Delta x \sum_{v=\frac{-(M-1)}{2}}^{\frac{M-1}{2}} s_c(f_n,\delta_v)\exp(i2\pi k_m \delta_v) \qquad \text{A.5.9}$$

If one substitutes for $s_c(f_n,\delta_v)$ from Equation A.5.8 into A.5.9, one obtains

$$W(f_n,k_m) = \Delta x \sum_{v=\frac{-(M-1)}{2}}^{\frac{M-1}{2}} \Delta t \sum_{u=\frac{-(N-1)}{2}}^{\frac{N-1}{2}} R_c(\tau_u,\delta_v)\exp(-i2\pi f_n\tau_u)\ \exp(i2\pi k_m\delta_v) \qquad \text{A.5.10}$$

which can be rewritten to yield

$$W(f_n,k_m) = \Delta t\Delta x \sum_{u=\frac{-(N-1)}{2}}^{\frac{N-1}{2}} \sum_{v=\frac{-(M-1)}{2}}^{\frac{M-1}{2}} R_c(\tau_u,\delta_v)\ \exp[-i2\pi(f_n\tau_u - k_m\delta_v)] \qquad \text{A.5.11}$$

Recalling Equations A.5.4 and A.4.29 one can see that $W(f_n,k_m)$ equals $s(f_n,k_m)$. Thus, the two-dimensional spectral density function may be computed by a double Fourier transform of the two-dimensional covariance function, i.e.,

$$s(f_n,k_m) = \Delta t\Delta x \sum_{u=\frac{-(N-1)}{2}}^{\frac{N-1}{2}} \sum_{v=\frac{-(M-1)}{2}}^{\frac{M-1}{2}} R(\tau_u,\delta_v)\exp[-i2\pi(f_n\tau_u - k_m\delta_v)] \qquad \text{A.5.12}$$

or it also may be computed by a <u>single</u> transform from the cross spectral density function, i.e.,

$$s(f_n,k_m) = \Delta x \sum_{v=\frac{-(M-1)}{2}}^{\frac{M-1}{2}} s_c(f_n,\delta_v)\exp(i2\pi k_m\delta_v) \qquad \text{A.5.13}$$

3. Relationship between cross spectral density functions and two-dimensional auto-covariance function.

Suppose one computes a two-dimensional function, called here $Y(\tau_u,\delta_v)$, by a Fourier transform of $s_c(f_n,\delta_v)$ according to:

$$Y(\tau_u,\delta_v) = \Delta f \sum_{n=\frac{-(N-1)}{2}}^{\frac{N-1}{2}} s_c(f_n,\delta_v)\exp(i2\pi f_n\tau_u) \qquad \text{A.5.14}$$

The inverse of Equation A.5.13,

$$s_c(f_n,\delta_v) = \Delta k \sum_{m=\frac{-(M-1)}{2}}^{\frac{M-1}{2}} s(f_n,k_m)\exp(-i2\pi k_m\delta_v) \qquad \text{A.5.15}$$

may be used to substitute in Equation A.5.14 to obtain:

$$Y(\tau_u,\delta_v) = \Delta f \sum_{n=\frac{-(N-1)}{2}}^{\frac{N-1}{2}} \Delta k \sum_{m=\frac{-(M-1)}{2}}^{\frac{M-1}{2}} s(f_n,k_m)\exp(i2\pi k_m\delta_u)\exp(i2\pi f_n\tau_u) \qquad \text{A.5.16}$$

Upon rearrangement, the right-hand side is seen to be identical to the right-hand side of Equation A.4.28. Therefore, $Y(\tau_u,\delta_v) = R(\tau_u,\delta_v)$ or, again writing A.4.28,

$$R(\tau_u,\delta_v) = \Delta f\Delta k \sum_{n=\frac{-(N-1)}{2}}^{\frac{N-1}{2}} \sum_{m=\frac{-(M-1)}{2}}^{\frac{M-1}{2}} s(f_n,k_m)\exp[+i2\pi(f_n\tau_u - k_m\delta_v)] \qquad \text{A.5.17}$$

Thus, the two-dimensional auto-covariance may be computed from a double Fourier transform of the two-dimensional spectral density function, or it may be computed by a <u>single</u> Fourier transform of the cross-spectral density

function according to Equation A.5.14, rewritten as:

$$R(\tau_u,\delta_v) = \Delta f \sum_{n = \frac{-(N-1)}{2}}^{\frac{N-1}{2}} s_c(f_n,\delta_v)\exp(i2\pi f_n \tau_u) \qquad \text{A.5.18}$$

VI. SUMMARY

The underlying principles of spectrum analysis are discussed. Beginning with the definition of a Fourier series, it is shown that a spectrum is a plot of the squared amplitudes versus frequency of the harmonics which contribute to the variance a time series. It is also described how the squared Fourier amplitudes are proportional to the spectral density function computed by a Fourier transform of the data. The spectral density function is also shown to be the Fourier transform of the more familiar auto-covariance function.

The discussion next considers two simultaneous time series and shows how the closeness of the relationship of and the phase angle between the two series may be assessed by computation of the cross spectral density function from Fourier transforms of the data from both series. The cross spectral density function is found to be the Fourier transform of the covariance function for the two series.

Two-dimensional, space-time spectral analysis is considered. Analogous to the one-dimensional case, it is shown that a two-dimensional spectrum is a contour surface of squared Fourier amplitudes versus frequency and wave number of the harmonics contributing to the variance of some entity in time and space. The squared Fourier amplitudes are shown to be proportional to a two-dimensional spectral density function which may be computed by a double Fourier transform of the data. The two-dimensional spectral density function is shown to be the Fourier transform of a two-dimensional auto-covariance function.

Lastly, it is shown that, if samples of time series are available for various points across a field, both the two-dimensional spectral density function and the two-dimensional auto-covariance function can be computed from the cross spectral density functional relationships among the points.

VII. LITERATURE CITED

Allen, L. H., Jr. 1968. Turbulence and wind speed spectra within a Japanese larch plantation. J. of Appl. Met. 7:73-78.

Bingham, C., Godfrey, M. D., and Tukey, J. W. 1967. Modern Techniques of Power Spectrum Estimation. IEEE Transactions on Audio and Electroacoustics AU-15(2):56-66.

Blackman, R. B. and Tukey, J. W. 1958. The Measurement of Power Spectra. Dover Publications, New York, 190 p.

Brigham, E. O. and Morrow, R. E. 1967. The Fast Fourier Transform. IEEE Spectrum 4(3):63-70.

Cooley, J. W. and Tukey, J. W. 1965. An Algorithm for the Machine Calculation of Complex Fourier Series. Math. Comput. 19:297-301.

Desjardins, R. L. 1967. Time Series Analysis in Agrometeorological Problems with Emphasis on Spectral Analysis. Canadian J. Plant Sci. 47:477-491.

Jenkens, G. M. and Watts, D. G. 1968. Spectral Analysis and Its Applications. Holden-Day, San Francisco, 525 pp.

Lumley, J. L. and Panofsky, H. A. 1964. The Structure of Atmospheric Turbulence. John Wiley and Sons, Inc., New York, 239 pp.

McBean, G. A. 1968. An investigation of turbulence within the forest. J. of Appl. Met. 7:410-416.

Panofsky, H. A. and Brier, G. W. 1958. Some Application of Statistics to Meteorology. The Pennsylvania State Univ., Univ. Park, Penn, 223 p.

Rodriguez-Iturbe, S. and Nordin, C. F. 1969. Some applications of cross-spectral analysis in hydrology: rainfall and runoff. Water Resources Res. 5:608-621.

Singleton, R. C. and Poulter, T. C. 1967. Spectral analysis of the call of the male killer whale. IEEE Transactions on Audio and Electroacoustics AU-15(2):104-113.

Stockham, T. G. 1966. High-speed convolution and correlation. Spring Joint Computer Conference. American Federation of Information Processing Societies Proc. 28:229-233. Spartan Books, Washington, D. C.

Tick, L. J. 1967. Estimation of coherency. In Harris, B. ed., Spectrum Analysis of Time Series. John Wiley and Sons, Inc., New York, 319 pp.

Welch, P. D. 1967. The use of the fast Fourier transform for the estimation of power spectra: A method based on time averaging over short, modified periodograms. IEEE Transactions on Audio and Electroacoustics AU-15(2):70-73.

UNCLASSIFIED
Security Classification

DOCUMENT CONTROL DATA - R & D

(Security classification of title, body of abstract and indexing annotation must be entered when the overall report is classified)

1. ORIGINATING ACTIVITY *(Corporate author)* Microclimate Investigations, SWC-ARS-USDA Bradfield Hall; Cornell University Ithaca, New York 14850	2a. REPORT SECURITY CLASSIFICATION UNCLASSIFIED 2b. GROUP

3. REPORT TITLE

EFFECTS OF AIR TURBULENCE UPON GAS EXCHANGE FROM SOIL
with appendix
~~BASIC CONCEPTS OF SPECTRAL ANALYSIS BY DIGITAL MEANS~~

4. DESCRIPTIVE NOTES *(Type of report and inclusive dates)*

Interim Report

5. AUTHOR(S) *(First name, middle initial, last name)*

B. A. Kimball and E. R. Lemon

6. REPORT DATE November 1969	7a. TOTAL NO. OF PAGES 188	7b. NO. OF REFS 50
8a. CONTRACT OR GRANT NO. Cross-Service Order 2-68 b. PROJECT NO. c. DA Task 1T0-61102-B53A-17 d.	9a. ORIGINATOR'S REPORT NUMBER(S) USDA-ARS-SWC No. 405 and 406 C.U.Research Report No. 870 and 870A 9b. OTHER REPORT NO(S) *(Any other numbers that may be assigned this report)* ECOM 2-68I-4 and ECOM 2-68I-5	

10. DISTRIBUTION STATEMENT

Distribution of this document is unlimited

11. SUPPLEMENTARY NOTES	12. SPONSORING MILITARY ACTIVITY U. S. Army Electronics Command Atmospheric Sciences Laboratory Fort Huachuca, Arizona

13. ABSTRACT

An instrument to measure the rate of gas movement from beneath the surface of soil or other porous media was constructed. Subsequent measured rates of gas movement from beneath surface coverings of coarse and fine gravel, very coarse and medium sand, Chenango silt loam and straw were correlated against concurrent measurements of wind and air pressure fluctuations. At a depth of 2 cm gas movement in silt loam was not significantly affected by air turbulence but in coarse gravel was increased 10-fold by wind velocities of 400 cm/sec. Intermediate effects were observed for media of intermediated pore sizes.

Mathematical equations for calculation of soil air mass flow are derived. They are based upon the spectrum of air pressure fluctuations at the ground surface. Air pressure in the field was measured during both day and night with and without a corn crop. The spectra of air pressure were calculated and all were roughly straight lines with a slope of about -6/3 on a log-log plot. Spectral density decreased from 10^{8} to 10^{-1} μbar^2/cycle/sec over a frequency range from 10^{-4} to 10^{2} cycle/sec. Soil air mass flow was calculated from the spectra for several soils. Using previous work, an attempt was made to evaluate the increase of soil gas movement beyond diffusion from the soil air mass flow. The predicted increases in soil gas movement were lower than the observed increases; several reasons for the discrepancy are discussed.

Spectral density, Fourier transformation, auto-covariance, cross spectral density, cross-covariance, and other concepts of spectral analysis are discussed at an elementary level in the appendix.

DD FORM 1 NOV 65 1473 REPLACES DD FORM 1473, 1 JAN 64, WHICH IS OBSOLETE FOR ARMY USE.

UNCLASSIFIED
Security Classification

14. KEY WORDS	LINK A ROLE	LINK A WT	LINK B ROLE	LINK B WT	LINK C ROLE	LINK C WT
Soil - Mass flow						
Soil - Diffusion						
Soil - Dispersion						
Porous Media - Mass flow						
Porous Media - Diffusion						
Porous Media - Dispersion						
Air Pressure - Fluctuations						
Air Pressure - Spectrum						
Spectral Analysis - Methods						
Spectral Analysis - Concepts						
Spectral Analysis - Air Pressure						